

36
LEVEL II

ARO

14795.1-E

(12)

A STUDY OF THE EFFECT OF TERRAIN
ON
HELICOPTER NOISE PROPAGATION
BY
ACOUSTICAL MODELING

FINAL TECHNICAL REPORT

HARRY STERNFELD, JR.

MARCH 23, 1981

U.S. ARMY RESEARCH OFFICE

CONTRACT DAA629-78-C-0002

BOEING VERTOL COMPANY

DTIC
ELECTRONIC
APR 8 1981
C

AD A 097 626

DTIC FILE COPY

APPROVED FOR PUBLIC RELEASE,
DISTRIBUTION UNLIMITED.

81 4 13 053

THE VIEW, OPINION, AND/OR FINDINGS CONTAINED IN THIS REPORT ARE
THOSE OF THE AUTHOR(S) AND SHOULD NOT BE CONSTRUED AS AN OFFICIAL
DEPARTMENT OF THE ARMY POSITION, POLICY, OR DECISION, UNLESS SO
DESIGNATED BY OTHER DOCUMENTATION.

REPORT DOCUMENTATION PAGE		READ INSTRUCTIONS BEFORE COMPLETING FORM
1. REPORT NUMBER	2. GOVT ACCESSION NO.	3. RECIPIENT'S CATALOG NUMBER
	AD-A 097 626	
4. TITLE (and Subtitle)	5. TYPE OF REPORT & PERIOD COVERED	
A Study of the Effect of Terrain on Helicopter Noise Propagation by Acoustical Modeling	9 Final Report	
7. AUTHOR(s)	6. PERFORMING ORG. REPORT NUMBER	
10 Harry/Sternfeld, Jr	DAAG29-78-C-0002 N	
8. PERFORMING ORGANIZATION NAME AND ADDRESS	9. CONTRACT OR GRANT NUMBER(s)	
Boeing Vertol Company P.O. Box 16858 Philadelphia, Pa. 19142	18 ARO	
10. PROGRAM ELEMENT, PROJECT, TASK AREA & WORK UNIT NUMBERS	11. REPORT DATE	
19 24795.2-E	12 5/6/81	
11. CONTROLLING OFFICE NAME AND ADDRESS	13. NUMBER OF PAGES	
U. S. Army Research Office Post Office Box 12211 Research Triangle Park, NC 27709	11 54	
14. MONITORING AGENCY NAME & ADDRESS (if different from Controlling Office)	15. SECURITY CLASS. (of this report)	
13 DAAG 29-78-C-0002	Unclassified	
16. DISTRIBUTION STATEMENT (of this Report)	15a. DECLASSIFICATION/DOWNGRADING SCHEDULE	
Approved for public release; distribution unlimited.		
17. DISTRIBUTION STATEMENT (of the abstract entered in Block 20, if different from Report)		
NA		
18. SUPPLEMENTARY NOTES		
The view, opinions, and/or findings contained in this report are those of the author(s) and should not be construed as an official Department of the Army position, policy, or decision, unless so designated by other documentation.		
19. KEY WORDS (Continue on reverse side if necessary and identify by block number)		
Acoustical Modeling Helicopter Noise Noise Propagation Detection		
20. ABSTRACT (Continue on reverse side if necessary and identify by block number)		
An experimental program was conducted to evaluate the applicability of acoustical modeling techniques to study the effects of terrain on helicopter noise propagation.		
Comparison of model results with flyover data of a full scale UH-1 helicopter showed very good correlation with 500 ft altitude data and moderately good correlation with 50 ft altitude data.		
(over)		

20. ABSTRACT (continued)

Model studies of the effects of the blocking and channeling of sound by barriers, such as hills, shows good correlation with expected results for simple cases with the model providing useful results for more complex cases.

Further full scale verification is recommended to further exchange confidence in the modeling technique for application to helicopter detection studies.

TABLE OF CONTENTS

	PAGE
1.0 INTRODUCTION	1
2.0 MODEL DEVELOPMENT	2
2.1 General Approach	2
2.2 Sound Sources	3
2.3 Instrumentation	4
2.4 Model Construction	5
3.0 MODEL VERIFICATION	6
3.1 Model Test	7
3.2 Correction for Atmospheric Attenuation	7
3.3 Correction for Directivity	7
3.4 Validation Test Results	8
4.0 BARRIERS	10
5.0 CHANNELING OF SOUND	14
5.1 Line of Sight	14
5.2 Bends	17
6.0 CONCLUSIONS AND RECOMMENDATIONS	18
REFERENCES	19
PERSONNEL	21
ILLUSTRATIONS	22

Accession For	
NTIS GRA&I	<input checked="" type="checkbox"/>
DTIC TAB	<input type="checkbox"/>
Unannounced	<input type="checkbox"/>
Justification	
By _____	
Distribution/	
Availability Codes	
Dist	Avail and/or Special
A	

1.0 INTRODUCTION

The increasing use of helicopters in tactical situations has led to the development of two types of low altitude operations referred to as 'Nap of the Earth' Flying and 'Contour Flying'. In contour flying the helicopter operates at altitudes which are above tree-top level but generally lower than that of the main terrain features such as hills. Nap of the Earth operations are conducted at even lower altitudes where the helicopter is often flying below tree-top level using the trees and small terrain features to hide behind. The purpose of such techniques are to minimize radar, visual, and hopefully aural detection.

In considering aural detection, there are three major elements; noise generation at the source, propagation to the observer, and detection and recognition of the signal. The subject of helicopter noise generation is very complex and has been the subject of considerable study for several years. A comprehensive review of the state of this particular art can be found in several publications such as Reference 1. Detection of helicopters by aural preception, although not studied in as great detail as noise generation, had also been the subject of research programs such as those reported in Reference 2, 3, 4, and 5.

Up to the present time, the studies of propagation of aircraft noise through the atmosphere and over terrain have concentrated on airplane noise where the aircraft is operating at substantial heights above the ground and Reference 6 describes a generally accepted method for calculating atmospheric attenuation for this situation. The unique problem associated with helicopter operations is that the noise source (the helicopter) is not remote from the terrain but actually operating in it such that the ground surfaces can act as acoustical barriers and/or reflectors thereby attenuating or amplifying the noise received at the observer compared with that which would be expected if there were only a direct (line of sight) path from source to receiver. Figure 1 illustrates some of the important effects which must be considered in accounting for terrain effects when predicting the aural detection of helicopters.

The development of prediction techniques for the effects of terrain on helicopter sound propagation would be extremely difficult and costly if one were to attempt the traditional approach of correlation of analytical prediction with full scale test data. Systematic variations in terrain features, such as changing surface impedance without changing the terrain geometry, or changing the width of a 'hill' without altering its height are virtually impossible. Even the detailed description of terrain, to any degree finer than a good contour map, would require an inordinate amount of effort and resources. It is for these reasons that acoustical modeling

techniques, such as have been employed for architectural acoustical studies, highway noise studies, and airport noise studies, presents a unique capability for conducting the desired investigation.

The objectives of this program were to adapt existing acoustical modeling techniques so that they would be optimum for application to helicopter noise propagation, verify the applicability, and then use the modeling approach to evaluate the sensitivity of the noise propagation to systematic changes in 'terrain'.

2.0 MODEL DEVELOPMENT

2.1 General Approach

An acoustical model is a physical model in which the scaling factor is wavelength. For example, if one constructs a model which is 1/X times the size of full scale, then one must use noise sources whose wavelengths are 1/X times that of the noise source to be studied. Since wavelength is related to frequency by:

$$\lambda = \frac{c}{f}$$

Where f = Frequency
 c = Speed of sound
 λ = Wavelength

It is simpler to think of model scaling as a 1/Xth scale model requires noise sources whose frequencies are X times that of the full scale noise source. In a similar manner, acoustical properties of the materials used to construct a model must also be frequency scaled. For example, if a full scale material has an absorption coefficient of .7 at 1000 Hz, a 50th scale model material would be required to have an absorption coefficient of .7 at 50,000 Hz.

The physical scale of the model is dictated by two parameters: the size of the full scale situation and the room available for the model. In the case of this program, studies of helicopter detection have indicated that the critical range for aural detection ranges from about 1/2 to 2 kilometers, although with very quiet ambient conditions certain helicopters can be detected at considerably greater distances. The model itself may be of any size as limited by practical economic considerations and available room size. As a practical matter, it is desirable to keep the model size to one where all parts could be reached without walking on the model surface and to a size which would not require extraordinary sized rooms, so that these techniques could be employed at reasonable cost. It was decided, for this study, to limit the model long dimension to 16 ft. since the ratio of 2 km to 16 ft. is 410 to 1 an acoustical scale of 400 to 1 was selected for these experiments as being typical of that which might be employed for helicopter detection studies. It should be pointed out that most acoustical modeling which has been performed to date has employed

scales of 100 to 1 or less and in this aspect alone the subject study is pushing the state-of-the-art.

Two types of measurement techniques are generally employed in acoustical modeling. The first technique uses steady state noise such as a loudspeaker or an air jet as a source and the resultant sound pressure levels are measured at various locations of interest on the model. While this method does provide information on amplification or attenuation of sound, it does not give any insight as to the relative contributions from multiple propagation paths, if they exist. If a very short duration impulsive source, such as an electric spark is used, the separate arrivals of the directly radiated and reflected time paths can be sensed and separated to provide such information. Both techniques, as they were applied to this program, will be described more fully in the remainder of this section.

2.2 Sound sources

A sound source can be described by three primary characteristics: its spectrum in the frequency domain, its patterning in the time domain (steady, random or periodic) and its spatial directivity. An ideal model noise source would be scaled by the inverse size scale of the model, in the frequency and time domains, and should replicate the directivity of the original source. In addition, it may be desirable that the physical size of the model sound source also be somewhat in scale. A helicopter rotor acoustical signature is extremely complex with respect to all of the required descriptors. Figure 2 (from Reference 7) depicts several sources of helicopter rotor noise classified by their time domain characteristic of periodic or broadband. Figure 3 illustrates the spectra and waveforms associated with several of the periodic sources. Directivity of rotor noise is also a function of the generating mechanism. Impulsive noise, for example, tends to maximize in, or near, the plane of the rotor while rotational and broadband sources are greatest below the disk. The cases which are of interest in studying helicopter detection are those which are generally impulsive in waveform and whose spectra are dominated by harmonic response. Some initial effort was made to develop a model sound source which would replicate the full scale signature using a frequently shifted magnetic tape recording of an actual helicopter as a source. In the first case, the source was used to drive a condenser microphone as a speaker. Although fidelity was reasonable, the signal was too weak for practical use at distances greater than about one foot. Two other attempts were made using piezoelectric crystals as the transducer. In one case the vibrating crystal was used to drive a small piston inside a casing and in the other, the exposed faces of a 3 inch diameter and a 6 inch diameter crystal were used as pressure sources. Neither the vibrator nor the 3 inch crystal provided sufficient acoustical power, and all three systems exhibited such marked resonance characteristics

that it became apparent that excessive manipulation of the test results would be required, and in fact, one would be better off with a powerful noise source with a rather smooth spectrum. The data could then be read out at any desired frequency. Such a procedure is valid if it can be assumed that in detecting sounds people sense on sound pressure level and frequency but not on the interrelationship between levels at different frequencies. Another way of stating the above is that detection is amplitude and frequency dependent but is not dependent on phasing between frequency components. Fortunately, this turns out to be the case as was determined by Fidel and Pearsons (Reference 8) and more recently verified by A. Ahumada of the Stanford Research Institute who specifically studied the detection of the HU-1 helicopter and found harmonic phasing not significant. In fact, the procedures for predicting detection (References 9 and 10), which have been verified by field tests (References 11 and 12), do not consider a spectrum definition which is any finer than one-third octave, or at very low frequencies the critical bandwidth of the ear.

It was therefore decided to use a broadband noise source of sufficient intensity to do the job and to read the data at the frequencies which corresponded to the appropriate helicopter rotor harmonics. An air jet, similar to one which had been designed at MIT consisting of four impinging nozzles, was constructed (Figure 4a). When operating with 80 psi of air pressure, the level with a useful spectrum leveled out to 80 KH² (shown in Figure 4b). The impulsive source was an electric spark generated by a Grozier Technical Systems Inc. GTS51 Spark Generator (Figure 4c) which discharges a high voltage capacitor when the electrode gap is ionized by a 30 KV low energy spark. The resultant acoustical signature is an extremely short duration 'N' wave.

2.3 Instrumentation

Data was measured using a Bruel and Kjaer 4135 1/4 inch diameter condenser microphone mounted on a Type 2619 cathode follower powered by a Type 2807 Power Supply. The 1/4 inch microphone was selected as an optimum considering the trade-off between frequency response and sensitivity. Frequency spectra from the air-jet source were obtained using a Federal Scientific UA-500A "Ubiquitous" Spectrum Analyzer which produces spectra such as that illustrated in Figure 4b. When required, a Federal Scientific Model 30A Range Translator was used to isolate and expand specific portions of the spectrum. This was done not only to obtain finer frequency resolution but to permit greater amplification of the high frequency end of the spectrum without saturating the higher amplitude lower frequency data.

While the frequency analysis system used with the air-jet was relatively conventional, the analysis equipment used to extract information from the spark signal is more specific to this

particular measurement. The elements of the system perform the following functions: the signal from the microphone power supply is amplified using a low noise, high gain scaling amplifier (Grozier Model GTS20) and the signal amplified as required to provide an input for a Grozier Model GTS33 Waveburst Processor which has the capacity to separate the sequential impulses through variable short term averaging and, if desired, to measure the energy of each impulse. The Waveburst Processor also incorporates a trigger and delay system which is used to activate the system when the spark is generated but blanks out the reception of the electromagnetic energy associated with the spark generation while admitting the more slowly traveling acoustical energy. The output of the Waveburst Processor was captured and measured using a Nicolet Model 2090-III 'Explorer III' Oscilloscope. This device digitizes the input signal, captures it in a memory, and displays the information on a screen. Digital readouts of the amplitude (voltage) and time corresponding to any point on the signal can be obtained by suitable positioning of the cursor(s). The device can also be used to expand the data along either axis to enhance reading accuracy. Disk storage is also available for preserving the records. With this device, reading accuracies to .001 milli-second and .1 millivolt are easily obtainable. Typical output displays are shown in Figure 17.

2.4 Model Construction

In order to conduct a successful acoustical modeling experiment, it is necessary to ensure that there are no paths, extraneous to the model, by which acoustical energy can travel from the sound source to the microphone. Such paths might include reflections of room walls and ceilings, lighting fixtures, equipment in the room, or the model support structure. This program was carried out in a test chamber of the Boeing Vertol Acoustical Laboratory which is a large (35' x 17' x 20') room with all four walls and ceiling lined with an acoustically absorptive treatment and a carpeted floor. The chamber also has its own air conditioning system incorporating mufflers to minimize ambient noise. The criteria used to declare the room satisfactory was that using the spark test technique any reflection from the room must be at least 20 dB below that of the direct path. This test chamber was adequate by itself but when the plywood necessary for building the model base was introduced, these surfaces were unacceptably reflective even when covered with several layers of very fine filament (PF105) fiberglass. A satisfactory solution was found by constructing a second inner surface of "foamcore", a paper faced rigid foam spaced by an 'eggbox' separator from the plywood and then lining this inner surface with 3" layers of 1/2" thick fiberglass. Figure 5a illustrates this final configuration the result of a spark test, within the enclosure showed it to be essentially anechoic and therefore satisfactory for further testing. Selection of model materials to simulate terrain has not been

reduced to a rigorous scientific basis and in fact, the best proof of proper selection probably lies in correlation between model and full scale data. As discussed in Reference 13, the absorption of acoustical energy by the ground is probably of less importance than the impedance which determines the phasing between the directly propagated path and the ground reflection. This is illustrated in Figure 6. In order to show the effects of surface impedance, two materials were selected: the first was very high impedance steel plate and the second was a low impedance material. In as much as possible, it was desired to make this lower impedance material a reasonable scaled approximation for relatively firm ground such as was on the surface of the airfield when measurements were made. The absorption coefficient and/or acoustic impedance of ground is very difficult to measure and generally somewhat meaningless since most natural surfaces are far from homogeneous. Work such as References 14 and 15, however, indicate that maximum attenuations due to ground effects of the range of 10 dB to 15 dB might be expected. An experiment was set up in which the spark was used as a source and the difference between direct and reflected path sound pressure levels measured. Several candidate materials were tested including cork, 1/4" foam, poster board, plywood and two types of fiberglass insulating board. Of these materials, the one which most closely matched the desired characteristic was Owens Corning Linear Glass Board. This material consists of fiberglass fibers with a binding material which forms a moderately rigid board and faced on one side with a porous protective facing.

3.0 MODEL VERIFICATION

The model, and modeling techniques, were verified, for application to helicopter noise studies, by comparison of model and full scale data of a HU-1 helicopter flying over open terrain at altitudes of 50 ft. and 500 ft. In making such comparisons, the following adjustments are made to the model data:

$$SPL_c = SPL_m + \mathcal{J}_A + \mathcal{J}_D$$

Where

- SPL_c = Corrected Model Sound Pressure Level
- SPL_m = Measured Model Sound Pressure Level
- \mathcal{J}_A = Correction For Atmospheric Attenuation
- \mathcal{J}_D = Correction For Directivity

3.1 Model Test

Since the terrain being modeled in this case was flat ground with line of sight propagation path, the model which is illustrated in Figure 7a was simply a flat surface 4' wide by 16' long thus permitting a full scale approach distance of about 6000'. The microphone was mounted at one end of the surface with its diaphragm vertical and in the plane determined by the 'flight path' and the normal to the ground plane. In this manner microphone directivity sensitivity did not vary as during the 'flyover'. The microphone center was .15" above the surface which corresponded to the 5' height of the full scale microphone. It must be recognized, however, that in the modeling scale being used, the microphone cartridge diameter represented 8.3'. The air-jet was placed at the appropriate height above the ground surface and spectra of the type illustrated in Figure 4 were recorded for each of twenty 'aircraft positions' until the source was directly over the microphone.

3.2 Correction for Atmospheric Attenuation

It is well known that as sound propagates through the atmosphere its sound pressure level in the far field decreases by 6 dB per doubling of distance due to simple spreading of the energy over the surface of an expanding sphere plus additional losses due to heat conduction and viscosity (classical absorption) and to molecular absorption which results from a vibratory relaxation process of oxygen and nitrogen molecules. A discussion of atmospheric losses can be found in References 3 and 6 along with tables for estimating these losses as a function of temperature and relative humidity. Atmospheric attenuation is very sensitive to frequency and the available tables do not cover the ultrasonic range which was employed in the modeling. In order to provide this information, tests were conducted by measuring the noise in incremental distances from one to sixteen feet from the source. This data, shown in Figure 8, indicates that between 1 and 3 ft. from the source the attenuation rate is greater than 6 dB per doubling of distance which is typical in the 'near field' where the noise generation cannot be considered as coming from a point source. Beyond 3 ft. the slope of the lower frequencies closely approaches the 6 dB per doubling of distance with increasing deviation as frequency increases. This data was used to correct the model data while the charts of Reference 6 were used for adjusting the full scale data.

3.3 Correction for Directivity

The directivity of the full scale helicopter harmonic noise was taken from the work of Schmitz and Boxwell (Reference 14) who measured free field noise around a HU-1H helicopter, in forward flight, by means of microphones mounted on a quiet airplane. Directivity of the model source (air-jet) was found to

be quite sensitive to the angle and alignment of the four small impinging air-jet tubes. It was not practical, however, to produce a model source as directional as the helicopter and so the tubes were positioned to provide as omnidirectional source as possible. Figure 8a, which compares the directivity of the helicopter harmonic noise with that of the model source, was used to develop the required corrections. An assumption implicit in this procedure is that on the helicopter all harmonic amplitudes have the same directivity. Since the generation of high amplitude harmonic noise is caused by discrete azimuthal functions, such as local blade-vortex intersections and/or the azimuth locations of highest resulting advancing tip speed, and do not occur randomly around that azimuth, such an assumption is not illogical.

3.4 Validation Test Results

Model testing was conducted to simulate flybys of a UH-1H helicopter at altitudes of 50' and 500' and a sideline distance of 200' in order to correspond with full scale data which was already available. The full scale data had been recorded at a quiet open airfield with closely mowed vegetation. Two terrain surfaces were used on the model in order to demonstrate impedance effects, one was a 'hard' metal surface and the other was the 'soft' linear fiberglass board discussed previously which it was thought would approximate the terrain.

The air-jet was located at increments along the 'flight path' corresponding to full scale increments of 90 meters as illustrated in Figure 7a. Figure 7b displays a typical spectra measured at the microphone and indicates how the spectrum could be read to predict the effects on rotor harmonic levels of desired helicopter.

The full scale data was reduced by playing the magnetic tape recording through a 1/3 octave band analyzer onto a strip chart recorder. One third octave bandwidth was selected because this is the basis for analytical detection predictions (References 9 and 10) This data was read at intervals corresponding to every 100 meters of aircraft location.

The data was reduced and corrected for atmospheric and directivity effects. Figure 9 shows a typical set of corrections and indicates the pronounced role of directivity, particularly at close range. The full scale data must be corrected in the time domain because although the aircraft position is initially correlated with the sound at the microphone, this is not its location at the time the sound was generated. The full scale data, therefore, must be retarded by the time which it took the sound to travel from the aircraft to the microphone.

Figures 10 and 11 present the results of the model validation test. Each figure shows the model test results as measured and corrected. Also shown is the time retarded full scale data. There is no direct relationship between the absolute amplitudes of the model and full scale data and they are to be compared only for trend. In order to aid such comparison, the full scale data has been normalized to the model data. The normalization points were selected as 500 meters in order to be far enough away to past the range of very rapid directivity changes and close enough to avoid excessive atmospheric or terrain effects. The data has been shown for the center frequencies of preferred octave bands but comparisons could have been made for any specific frequency such as that corresponding to a particular rotor harmonic. (Figure 7).

The general trend of sound pressure level variation with distance results from the trade-off between atmospheric attenuation and directivity. At low altitude the distance parameter dominates as the aircraft passes close to the microphone and the drop off due to directivity does not occur until the helicopter is almost overhead. At altitude, however, the directivity effect, which tends to maximize in the rotor plane, is relatively stronger and the maximum value occurs further away. The agreement between model and full scale data for the 500' altitude (Figure 11) is quite good.

The model hard surface data is higher than that with the soft surface. With a coincidence dip of the type discussed earlier, and illustrated in Figure 6, can be seen when the model had a hard surface. These points which are indicated (*) on Figure 11 are not evident with the 'soft ground' model nor in the data thereby verifying the selection of the glass board as a reasonable for simulation of ground impedance.

The match of full scale data with model data for low altitude flight (Figure 10) shows greater anomalies than does the higher altitude data. At low altitude, a dip in the full scale data occurs beyond about 1000 meters. This is believed to be due to the fact that the airfield at which the measurements were made bordered by a dense growth of high trees which blocked the line of sight to the helicopter at approximately that distance. Therefore, the low altitude comparisons will be considered valid within 1000 meters only. The discrepancies between model and test data appear to occur when the grazing incidence angle of the acoustic propagation becomes less than about 1° . At these low angles, extra terrain losses, due to vegetation, and scattering due to small objects becomes quite important and it appears that a more textured (but not lower impedance) terrain simulation might have improved the correlation. This might be achieved by using a grid or netting over the glass board to get more scattering at greater distance.

The coincidence dips and large variations in sound pressure level as the aircraft approaches the overhead location are of considerable importance to civil concerns, such as effects of ground surface on aircraft noise certification, because they affect the measured noise levels at or near their maximum levels. These conditions are of little interest to the question of detection, however, because the aircraft is not only plainly visible but the warning times are down to a very few seconds.

4.0 BARRIERS

The effect of thin barrier, walls on the attenuation of noise has studied quite extensively. Since barriers which are encountered in natural terrain formations such as hills and mountains are, if generally are extremely thick and without well defined edges. It was desired to employ acoustical modeling techniques to examine what happens as barriers deviate from the classical 'knife edge' and how one might approximate a wide barrier for analytical purposes.

These tests were conducted using the lined enclosure shown in Figure 5. Barriers were inserted to separate the source and microphone as illustrated in Figure 12. In the 400:1 modeling scale used previously the barrier simulated was 800' high, the source 200' from the ground and both the source and receiver (microphone) 2600' from their respective barrier faces.

Rectangular barriers simulating 13', 100', 200', 300', 400', and 500' were used along with a 500' wide barrier whose top was a 250' radius circle. The corresponding model dimensions will be used throughout the remainder of this discussion.

The test technique employed and illustrated in Figure 12 was as follows:

1. The spark generator was located at the source location S1 and the time for sound to travel over the barrier to the microphone was measured.
2. The spark was replaced with the air jet and a frequency spectrum at the receiver location was recorded.
3. The barrier was removed and the spark fired to determine the time for the shortest path from source to receiver.
4. The spark generator was then moved back until the time of the direct sound path equalled that of the path over the barrier determined in step 1 (point S2). This could be done to an accuracy of .001 millisecond or a distance of about .001 ft.

5. The spark was replaced with the air jet and a second spectrum obtained.
6. The difference in spectra obtained in steps 4 and 5 was the insertion loss of the barrier since all atmospheric propagation losses had been cancelled out by this procedure.

Figure 13a shows the spectrum received with no barrier in place while Figure 13B compares this with the spectra obtained with each of the walls. The results of the tests are tabulated in Table I which shows barrier attenuation as a function of frequency, the measured delay time, the speed of sound during the test, and the computed difference in path length.

In order to evaluate these results they were first compared with that which would be expected by calculation using the thin barrier theory of Maekawa (Ref. 16) who developed a relationship between barrier attenuation in the "Shadow Zone" and the Fresnel Number N where $N = \frac{2}{\lambda} (\Delta L)$

where λ $\hat{=}$ Wavelength
 ΔL $\hat{=}$ Difference between path over barrier and shortest path.

The attenuation due to a barrier using Maekawa's formulation is presented graphically in Figure 14a. In order to apply this to thick barriers a screen of 'equivalent height' was used as illustrated on Figure 14b. Using this approach attenuations would be predicted for each test as shown in Table II. A quick comparison of the test results of Table I and this simplified analytical approach yields poor correlation, with respect to both absolute value and sensitivity with frequency, and a better analytical simulation of the barrier must be sought.

The shortcomings of applying thin screen approaches to wide barriers have been recognized and discussed in papers such as Ref. 17. Following the thinking of Pierce but still using the attenuation data developed by Maekawa leads to the approach illustrated below:

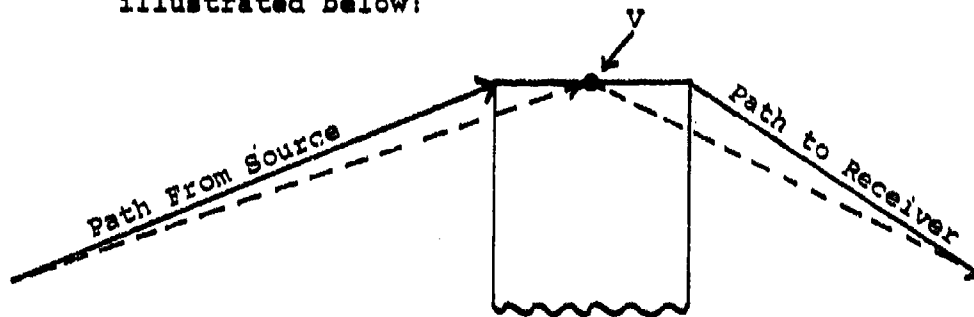


TABLE I - BARRIER INSERTION LOSS TEST RESULTS (A_b)

Barrier Thickness (Model Scale)

Frequency Khz	t=0	t=4"	3"	6"	9"	12"	15"	15**	15"
	SPL	SPL/ A_b							
10	50	46	45	48	41?	40?	-	-	-
20	66	53	55	50	45	46	-	-	-
30	77	60	61	60	58	58	48	29	50
40	75	64	64	58	58	52	50	25	52
50	70	60	55	53	50	48	47	23	48
60	66	52	50	46	43	41	40	26	41
70	65	48	42	42	36	37	-	-	36?
80	68	32	37	-	-	-	-	-	-
Delay Time-t(msec)	11.53	11.97	12.19	12.47	12.68	12.93	13.12	13.16	
Δt (msec)	0	.44	.66	.94	1.15	1.40	1.59	1.63	
Speed of Sound (ips)	13472	13486	13499	13511	13524	13536	13549	13549	
Δ Path Length (in)		5.934	8.909	12.700	15.553	15.792	21.54		

*Curved Top Barrier

TABLE Iia - CALCULATION OF PATH LENGTH -
'EQUIVALENT HEIGHT' BARRIER

h'	R	cs	ss	rs	sr	dl*
.4	78.24	24.48	80.39	78.16	186.82	2.03
3	79.73	24.80	81.92	79.27	189.11	2.08
6	81.44	25.21	83.67	80.56	192.11	2.12
9	83.18	25.61	85.43	81.88	195.11	2.17
12	84.62	25.96	86.94	83.38	198.11	2.21
15	86.57	26.42	88.98	84.43	171.11	2.27

*dl = (ss+rs)-sr

TABLE Iib - BARRIER ATTENUATION - 'EQUIVALENT HEIGHT' BARRIER

Barrier Thickness c FT/SEC	EQUIVALENT HEIGHT											
	4"		3"		6"		9"		12"		15"	
	N	Ab	N	Ab	N	Ab	N	Ab	N	Ab	N	Ab
10	3.0	20	3.1	20	3.1	20	3.2	20	3.3	21	3.4	21
20	6.0	22	6.2	22	6.2	22	6.4	22	6.6	23	6.8	23
30	9.0	23	9.3	23	9.3	23	9.6	24	9.9	24	10.2	24
40	12.0	24	12.4	24	12.4	24	12.8	24	13.2	25	13.6	25
50	15.0	25	15.5	25	15.5	25	16.0	26	16.5	26	17.0	26
60	18.0	26	18.6	26	18.6	26	19.2	27	19.8	27	20.4	27
70	21.0	27	21.7	27	21.7	27	22.4	28	23.1	28	23.8	28
80	24.0	28	24.8	28	24.8	28	25.6	28	26.4	28	27.2	28

Instead of treating the entire barrier as a refracting edge consider each corner separately with a virtual source located at the center such that the level at V is first calculated, using Maekawa's method based on propagation from the original source and then using these levels as the source for propagation to the final receiver. Calculations are shown in Table III.

A comparison of the measured attenuation with calculated values using this 'Virtual Point' concept are shown in Figure 15 and shows good correlation at the lower frequencies but overprediction at the higher end of the spectrum. Comparison of data for the square edged and rounded top barrier indicated no significant difference in attenuation.

5.0 CHANNELING OF SOUND

The term channeling of sound, as used in this report, is meant to describe situations, such as helicopters flying through valleys or canyons, where the acoustical energy is reflected back towards the line of flight instead of spreading unimpeded in the original direction of propagation.

Two conditions were evaluated, a straight channel in which the source and receiver maintained 'line of sight' and a channel with a ninety degree bend.

5.1 Line of Sight:

The model used was the same one used for the barrier tests with the barriers removed. The variables were the materials used to face the surfaces. The soft fiberglass (PF-105) was used at the ends of the model, being anechoic they simulated an infinitely long channel length. The materials used to face the floor and walls were similar to those used in the flyover verification test except that aluminum was used instead of steel for the 'hard' surface. Once again it was felt that the fiberglass board and metal surfaces would bracket the range which might be encountered with natural terrain. Tests were conducted with the walls vertical and sloped outwards so that the effect of this variable could be identified. Spark testing was conducted to determine the relative strength of the directly radiated path and the reflected paths. The air jet noise source was then 'flown down the canyon' by moving it in increments and measuring spectra at the receiver location, as was done with the verification tests. The test setup was as illustrated in Figure 16. The noise source was kept at an 'altitude' of 6" (200' full scale) and the flight path was down the centerline of the model. Unsymmetrical microphone locations were used so that different path lengths and delay times would result from reflections from the two walls and thus could be separated and identified. Figure 17 shows the results of spark measurements with three configurations of increasing reflectivity. In Figure 17a the direct path radia-

TABLE III - BARRIER ATTENUATION 'VIRTUAL POINT' METHOD

t	f	SV		RV		ZA
		N=25Δt	A _{REV}	N	A _{REV}	
4	10,000	.0037	4	.0141	5	9
	20,000	.0074	4	.0282	5	9
	30,000	.0111	4	.0423	5	9
	40,000	.0148	5	.0564	5	10
	50,000	.0185	5	.0705	5	10
	60,000	.0222	5	.0846	6	11
	70,000	.0259	5	.0987	6	11
	80,000	.0296	5	.1128	6	11
3	10,000	.089	7	.1067	7	14
	20,000	.118	7	.2133	7	14
	30,000	.177	7	.3200	8	15
	40,000	.236	7	.4266	8	15
	50,000	.295	8	.5332	9	17
	60,000	.354	8	.6400	10	18
	70,000	.413	9	.7466	11	20
	80,000	.472	10	.853	12	22
6	10,000	.114	7	.227	7	14
	20,000	.228	7	.452	10	17
	30,000	.342	8	.678	11	19
	40,000	.456	10	.904	12	22
	50,000	.570	10	1.13	13	23
	60,000	.684	11	1.356	13	24
	70,000	.798	11	1.582	14	25
	80,000	.912	12	1.808	15	27
9	10,000	.169	8	.359	8	13
	20,000	.337	8	.718	11	19
	30,000	.506	10	1.077	13	23
	40,000	.674	11	1.436	15	26
	50,000	.843	12	1.795	15	27
	60,000	1.012	13	2.154	17	30
	70,000	1.18	13	2.513	17	30
	80,000	1.349	14	2.872	19	32
12	10,000	.222	7	.508	10	17
	20,000	.443	9	1.016	13	22
	30,000	.665	11	1.524	14	25
	40,000	.880	12	2.032	16	28
	50,000	1.108	13	2.54	17	30
	60,000	1.330	14	3.049	18	32
	70,000	1.55	14	3.556	18	32
	80,000	1.773	15	4.066	19	34
15	10,000	.2708	7	.675	11	18
	20,000	.541	9	1.349	14	23
	30,000	.812	11	2.024	16	27
	40,000	1.081	12	2.693	17	29
	50,000	1.353	14	3.373	18	32
	60,000	1.622	14	4.048	19	33
	70,000	1.894	15	4.722	19	34
	80,000	2.163	16	5.400	19	35

tion is clearly evident at 4.73msec delay time, with one reflective surface (17b) the additional path appears, when two facing walls become reflective (17c) multiple paths arise from reflections back and forth between the two facing walls.

Figure 18 shows a typical set of spectra which were measured with a configuration employing one reflective sidewall. It is interesting to note that when the source was located 12 inches from the sidewall a very strong pattern typical of constructive and destructive interference appears with a separation of about 2200 Hz. This corresponds to a calculated interference interval of 1903 Hz as illustrated in Figure 19, and considering precision of measurement is probably reasonably close. At a greater distance from the wall (19") the frequency, as expected, decreases but it is not clear why the depth of modulation is so much less or why it is not evident with a distance of 26". At the very close distance of 2" the interference pattern does not appear because the frequency has become extremely high and this interval between dips exceeds the resolution limits of the analyzer.

The air jet noise source was 'flown' down the model canyon with the several configurations of ground and wall materials which were indicated in Figure 16. The test results for three frequencies of noise are presented in Figure 20 which shows that at close range the directly radiated path dominates (within about 500 feet full scale and that as distance increases the hardness of the terrain becomes more important with the level increasing significantly with increased terrain hardness. None of these trends is unexpected and but the model does demonstrate the great effect which terrain can exert on the sound pressure level at the observer. In general the level measured at the maximum distance with the 'hard' terrain would not be reached until the aircraft range was only one third that distance with the 'soft' terrain.

Since the configuration with high absorption throughout is essentially anechoic the effect of successively increasing the reflectivity of the setup can be obtained by subtracting the levels measured with the former configuration from the latter ones resulting in the amplifications shown in Figure 21. This is a good method to use with model testing since all directivity and distance attenuation effects are automatically cancelled out. An idea of the strengths of the various propagation paths was obtained by also 'flying' the spark and measuring the amplitudes of the successively time delayed impulses such as those illustrated in Figure 17. Figure 22 shows the results for two reflective cases. Although the spark results encompass all frequencies they contain some interesting information. It appears that the first reflection is almost as strong as the direct radiation and that all others, with the possible exception of the second, could be neglected but even if there were no reinforcement by any reflected paths the magnitude of difference

between most and least reflective configurations of 15 dB as measured with the air jet could not be accounted for by summing of acoustic ray propagation paths. Figure 22b demonstrates clearly that all higher order reflections involved the second wall.

Another way of looking at the situation of the canyon model as an enclosed room with absorption coefficients of 1.0 at the top and ends and absorption coefficients corresponding to the appropriate material and frequencies for the sidewalls and ground surfaces. Using the method for calculating total steady state sound energy density of Ref. 18 Section 10.14 to predict the buildup within a room yields the results shown in Figure 23. Considering that the room volume of the model is at least an order of magnitude smaller than the applications for which the method was developed and considering the simplistic assumptions which were made one ought not to expect too good an agreement. But the fact remains that the test results indicate a stronger effect of terrain absorption than would be expected.

The effect of sloping the walls outward at approximately 45° is shown in Figure 24. This is, of course, a more natural situation because truly vertical walls are rarely encountered in nature. Indications are that additional attenuation will be experienced at moderately close ranges but at large distances a vertical wall model may suffice. The condition shown is for the most reflective configuration and the effect of slope would be expected to be even less with more absorptive surfaces.

5.2 Bends

The line of sight model was converted to the configuration illustrated in Figure 25 which results in a considerably more complex experiment. The results shown in Figure 26 indicate that the attenuation due to the bend, which is very evident with soft terrain, can be virtually cancelled but if the walls are reverberent. It also shows that when flying at very low altitude the effect of the ground is less than that due to the bend but the ground provides considerable attenuation of line of sight propagation. It is also quite evident that these effects increase with frequency.

Curving the outer wall of the bend had little effect on the data simulating N.O.E. operation as shown in Figure 27 but Figure 28 reveals an interesting effect on the data which simulated 200 ft. flying. The effect of the curvature is to reflect the pressure waves, as illustrated, so that they tend to bend around the corner instead of being reflected back. That this is more effective on higher frequencies, of shorter wavelength is indicated by the data which shows that the level with the curved wall increases from a level below that of the square bend at 20 KHZ(50 Khz full scale) to considerably higher than the square bend at 60 Khz.

One of the propagation paths illustrated in Figure 24 is that diffracted over the edges of the 'canyon' rather than propagating around the bend. In order to determine the effectiveness of this path a lid was put on the approach leg of the model so that this path was blocked. The results (Figure 29) clearly show that with soft terrain the path over the edges of the 'canyon' was a very substantial one and also increased with frequency and that failure to consider such propagation paths could lead to major errors in predicting detection distances. Note that with hard terrain the paths through the model still predominate

6.0 CONCLUSIONS AND RECOMMENDATIONS

The work described in this report has demonstrated that acoustical modeling techniques can be applied to studies of the effects of terrain on the propagation of helicopter noise. Experiments to separate complex effects, which are virtually impossible to perform in full scale are very easy to do with models. Although the techniques themselves are general they can be tailored to prediction of any particular helicopter provided its acoustical spectrum and directivity are known, either from measured data or analytical prediction. The tests which were conducted pretty much bounded the range of acoustical impedance and absorption which would be encountered in nature and demonstrated very large effects on noise propagation.

The model verification was conducted only for the classically, simple case of flat, soft, terrain and for this case showed good results when 'flying' 500 ft. above the ground but only moderate correlation with nap of the earth data. The model approach shows strong promise but needs further verification by application to more complex full scale situations for which both data and description of the terrain are known. One of the major questions to be answered is the detail to which terrain features must be modeled).

More research is also needed into modeling materials for proper simulation of various types of terrain.

REFERENCES

1. Anon., Helicopter Acoustics, NASA Conference Publication 2052, May 1978.
2. Loewy, R. G., Aural Detection of Helicopters in Tactical Situations, Journal of the American Helicopter Society, October 1963, pp. 36-53.
3. Ollerhead, J. B., Helicopter Aural Detectability USAAMRDL Technical Report 71-33, Eustis Directorate, U.S. Army Air Mobility Research and Development Laboratory, July 1971 AD 730788.
4. Hartman, L., and Sternfeld, H., An Experiment in Aural Detection of Helicopters; USAAMRDL Technical Report 73-50, Eustis Directorate U.S. Army Air Mobility Research and Development Laboratory, December 1973, AD 917355L.
5. Scruggs, B. W., and Hampton, Kenneth D., An Analytical Rotor Tip Speed to Reduce Helicopter Acoustic Detection; USARL Technical Note TN-37; U.S. Army Applied Technology Laboratory, August 1979 AD A076961.
6. Anon., Standard Values of Atmospheric Absorption as a Function of Temperature and Humidity, SAE. ARP 866A, Society of Automotive Engineers, Inc., March 1975.
7. Pegg, R. J., A Summary and Evaluation of Semi-Empirical Methods for the Prediction of Helicopter Rotor Noises, NASA TM 80,200 December 1979.
8. Fidel, S., and Pearsons, K.; Study of the Audibility of Impulsive Sources NASA CR1598, May 1970.
9. Ollerhead, J. B., Helicopter Aural Detectability, USAAMRDL Technical Report 71-33, Eustis Directorate, U.S. Army Air Mobility Research and Development Laboratory, July 1971.
10. Ungar, E., et al, A Guide for Predicting the Aural Detection of Aircraft, AFFDL-TR-71-22 Air Force Flight Dynamics Laboratory, Air Force Systems Command, March 1972.
11. Hartman, L., and Sternfeld, H., An Experiment in Aural Detection of Helicopters, USAAMRDL Technical Report 73-50, Eustis Directorate U. S. Army Air Mobility Research and Development Laboratory, December 1973.
12. Wylie Laboratories Inc., Correlation of Actual and Analytical Helicopter Aural Detection Criteria, USAAMRDL-TR-74-102A Eustis Directorate, U. S. Army Air Mobility Research and Development Laboratory, January 1975.

13. Lyon, R. H., Acoustical Modeling Handbook, Massachusetts Institute of Technology.
14. Schmitz, F. A., and Boxwell, D. A., In Flight Far-Field Measurement of Helicopter Impulsive Noise; Journal of the American Helicopter Society; Volume 21 No. 4 October 1976.
15. Parkin, P. H. and Scholes, W. E., Propagation of Sound at Hatfield, Journal of Sound and Vibration Vol. 2, Pg. 353, 1965.
16. Anon, Acoustic Effects Produced by a Reflecting Plane, Society of Automotive Engineers AIR 1327, January 1976.
17. Maekawa, Z., Noise Reduction by Screens, Applied Acoustics, 1968.
18. Pierce, A. D., Diffraction of Sound Around Corners and Over Wide Barriers, Journal of the Acoustical Society of America Vol. 55 No. 5, May 1974.
19. Beranek, L. L., Acoustics, McGraw Hill, 1954.

PERSONNEL

The following scientific personnel participated in the conduct of this study:

Principal Investigator - Mr. Harry Sternfeld, Jr.

Experimental testing was conducted by:

Mr. Bernard Borek
Ms Lisa Richardson (Intern student M.I.T.)
Mr. Edward Schaeffer

Illustrations were prepared by:

Mr. Mark Miller (Co-op student Widener College)

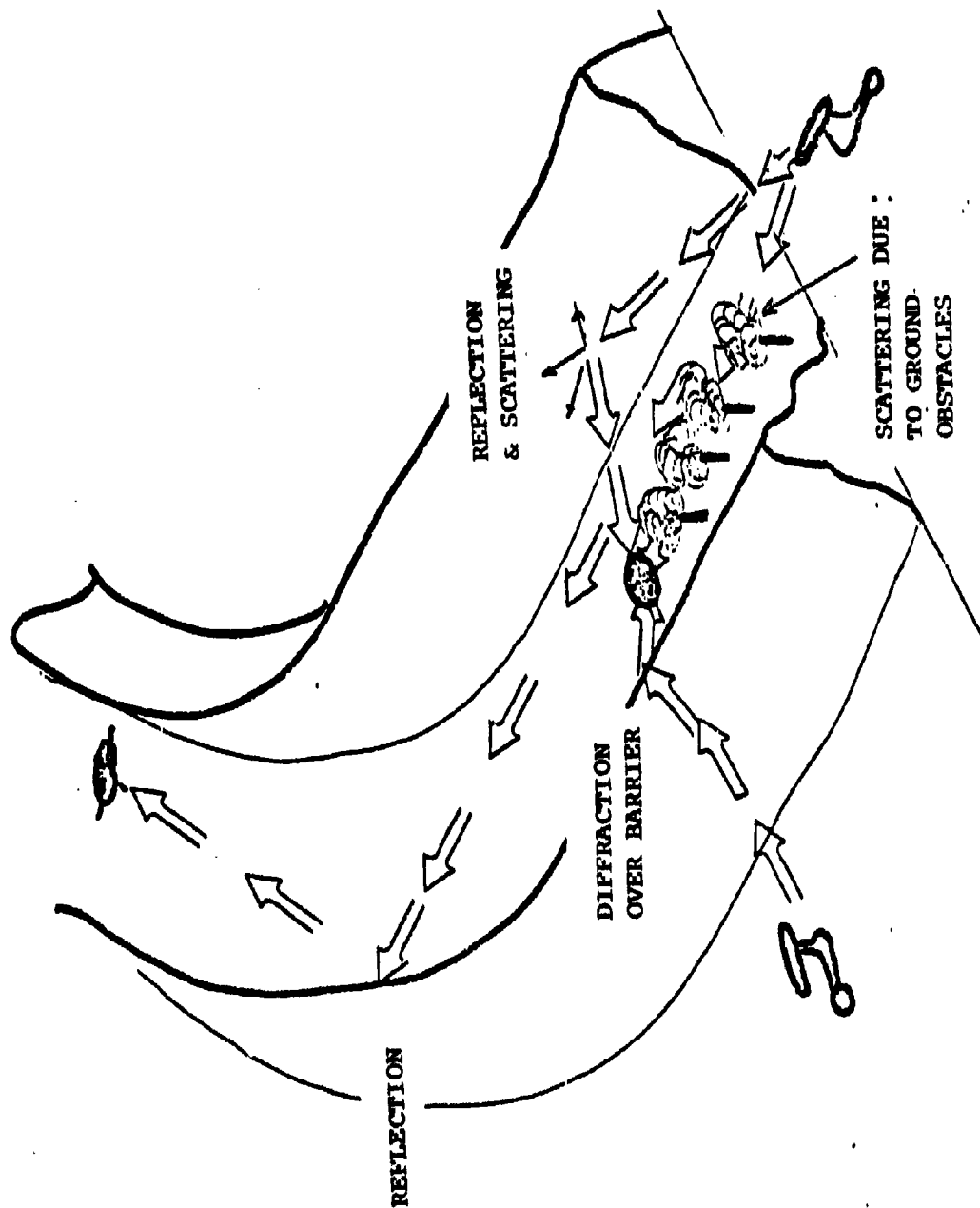


Figure 1 Effect of Terrain on Helicopter Noise Propagation

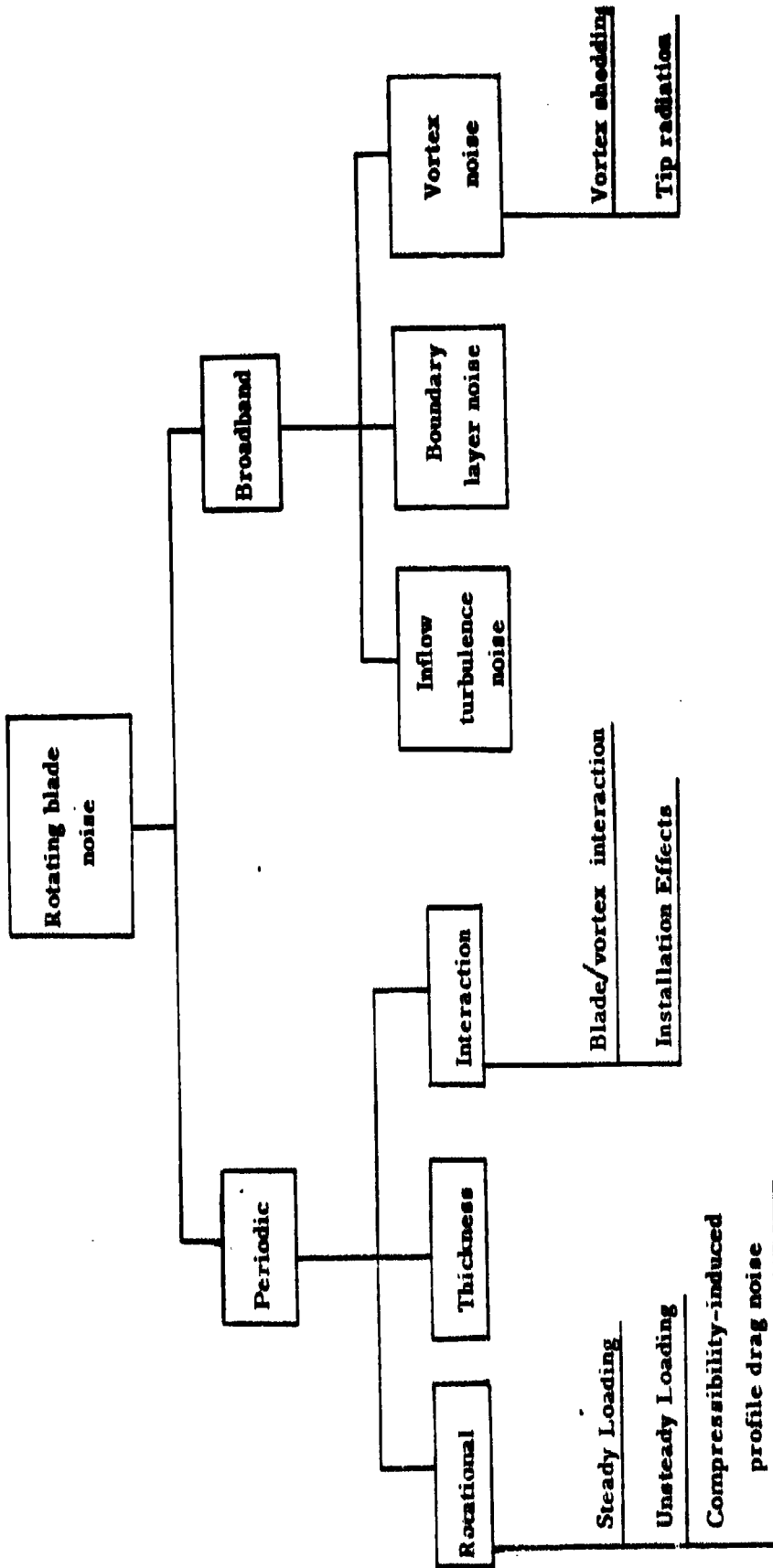


Figure 2 Block diagram of various noise components. (From Ref 7)

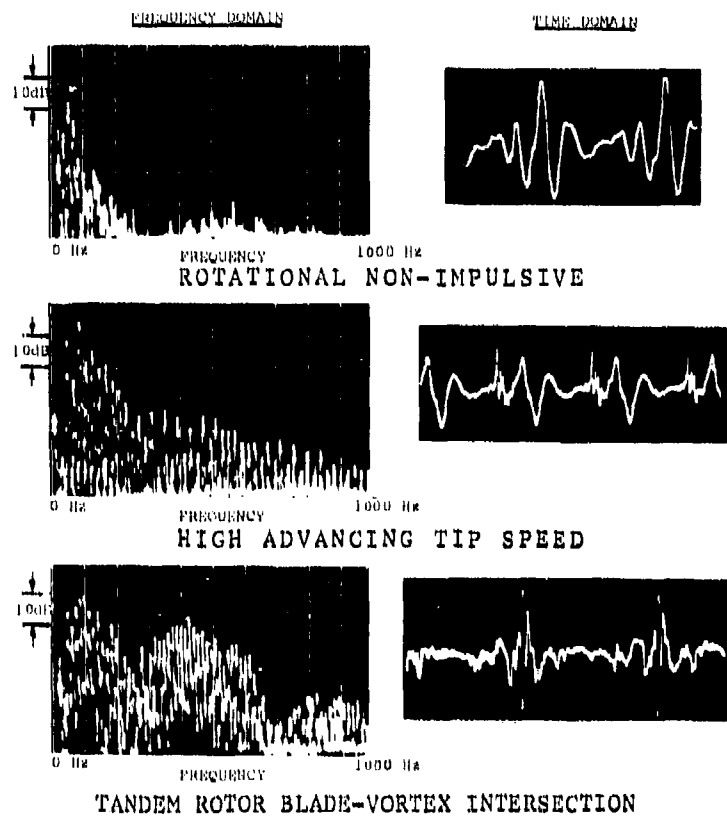
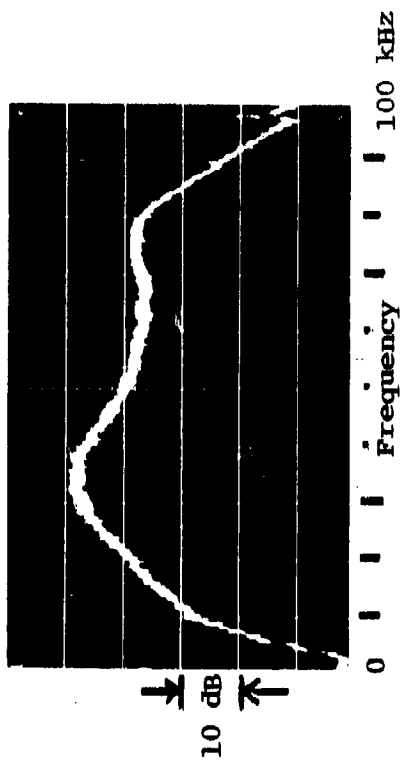


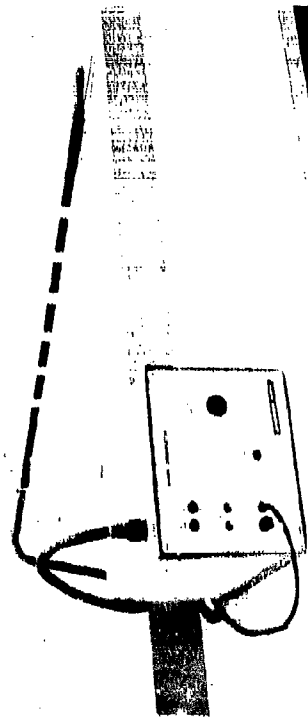
FIGURE 3. ACOUSTICAL SIGNATURES OF HARMONIC ROTOR NOISE



(a) Air Jet



(b) Air Jet Spectrum

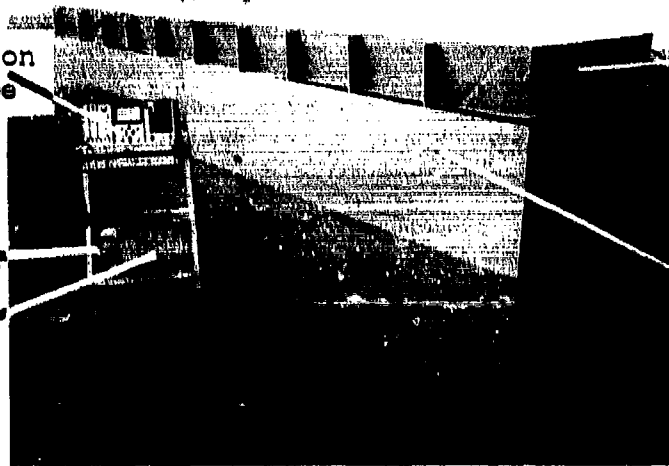


(c) Spark Generator

Figure 4-Model Noise Sources

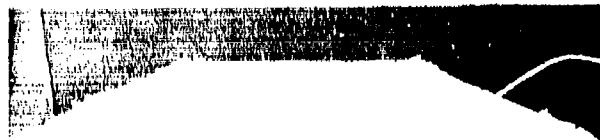
Spark Instrumentation
Storage Oscilloscope

Scaling Amplifier
Wave Burst
Processor



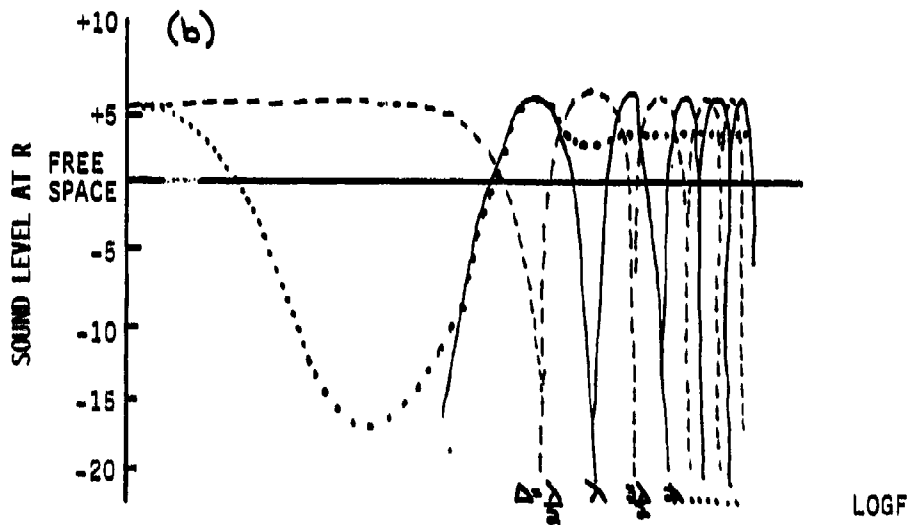
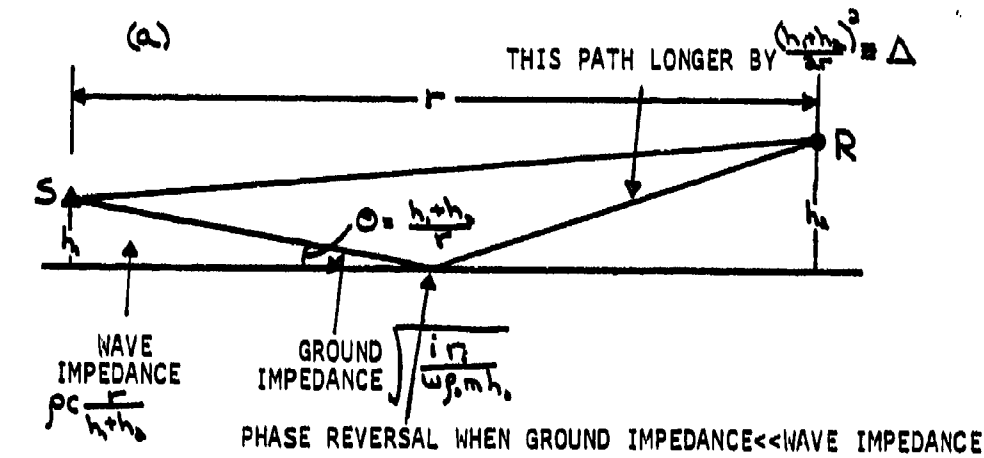
Inner
Isolating
Structure

Outer
Support
Structure



Soft
Fiberglass
Anechoic
Lining

Figure 5 Model Construction



- GROUND IMPEDANCE \gg WAVE IMPEDANCE
- GROUND IMPEDANCE \ll WAVE IMPEDANCE
- EXPECTED LEVEL RELATIVE TO FREE SPACE

Figure 6 SOURCE-RECEIVER ARRANGEMENT LEADING TO GROUND EFFECT AND THEORETICAL VALUES OF EXCESS ATTENUATION (REDRAWN FROM REF-13)

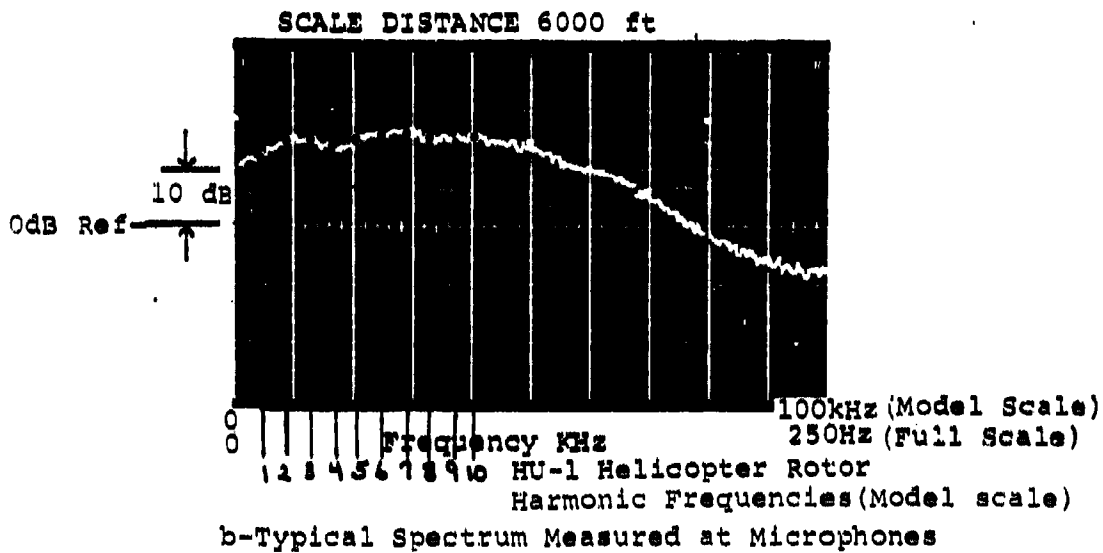
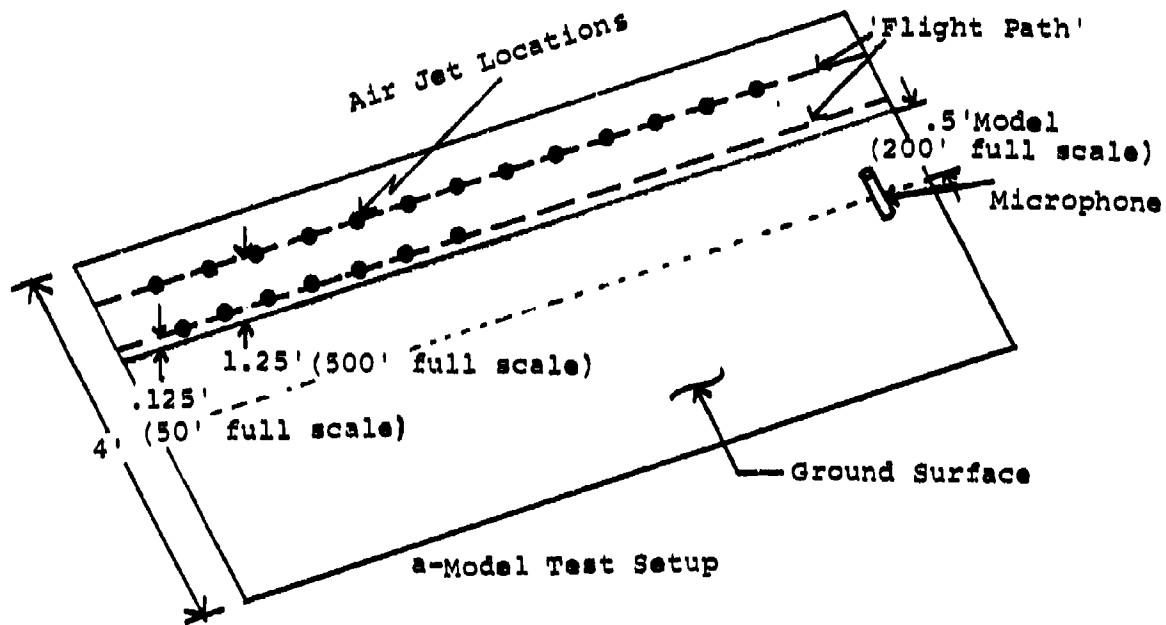


Figure 7 Validation Test

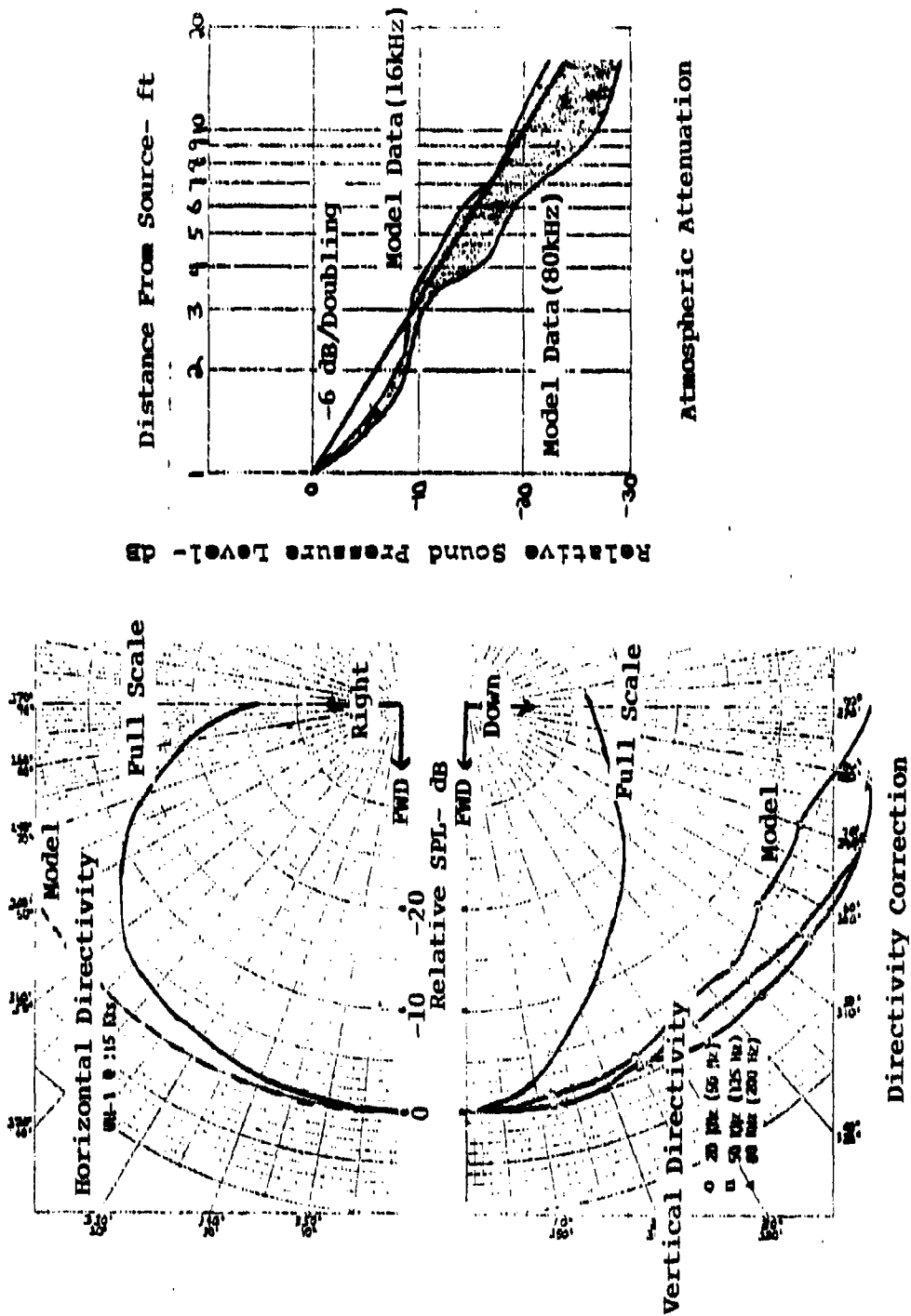


Figure 8 -Directivity and Atmospheric Corrections

200 Hz
500' Alt
Soft Terrain

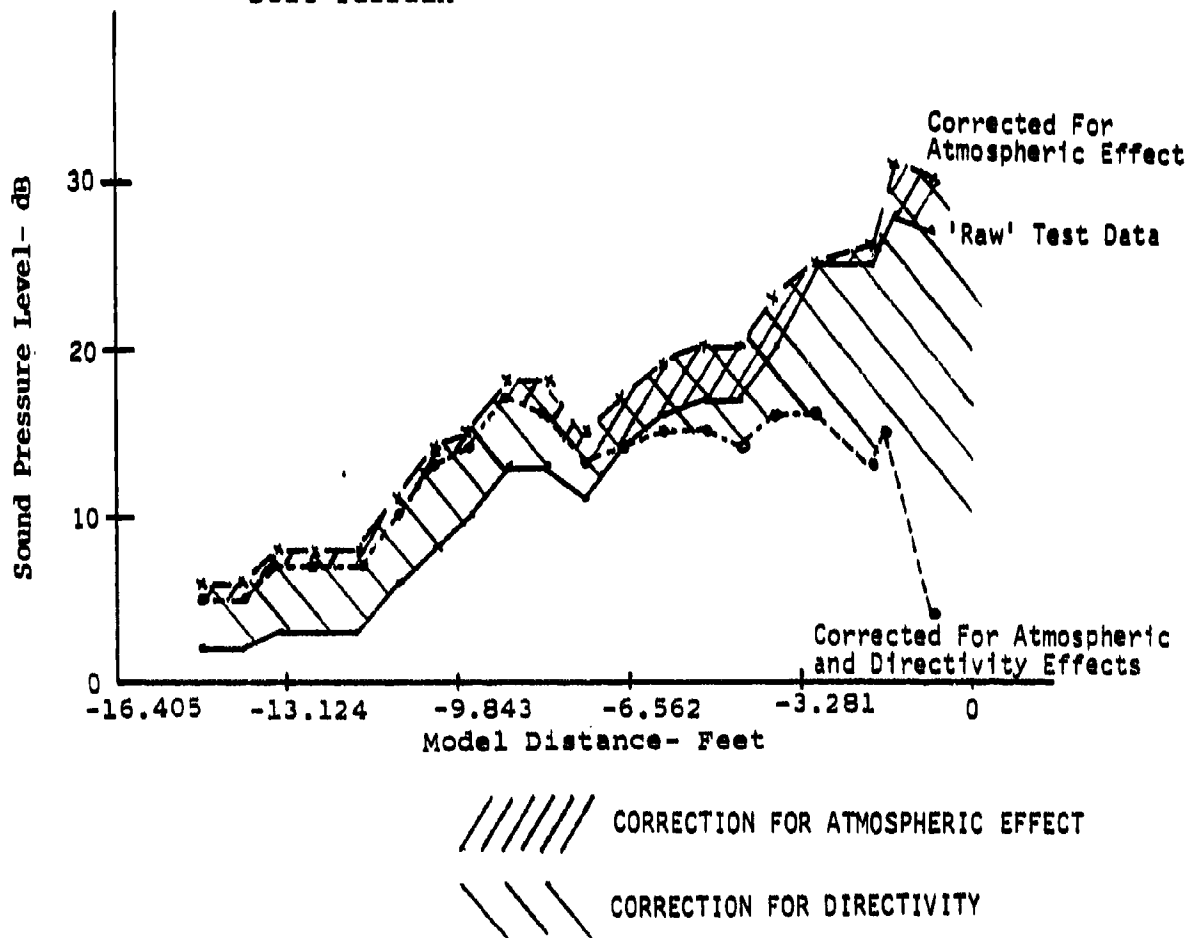
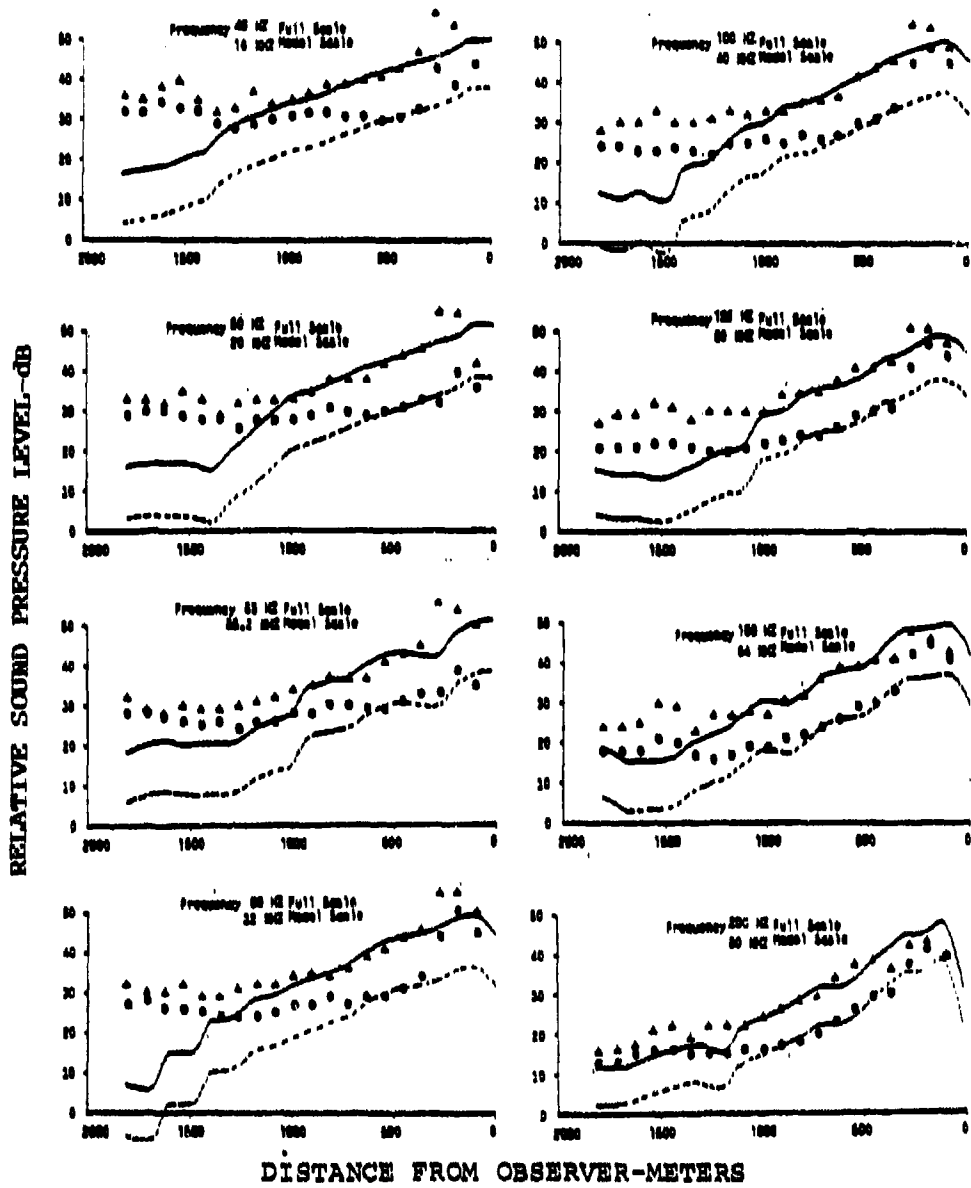


Figure 9-Model Data Corrections



RELATIVE SOUND PRESSURE LEVEL-DB

DISTANCE FROM OBSERVER-METERS

▲ 'Herd Ground'
 ○ 'Soft Ground'
 — Full Scale Data
 - - - (Normalized to Test Data)

Figure 10-Model Validation Test Results-50 ft Altitude

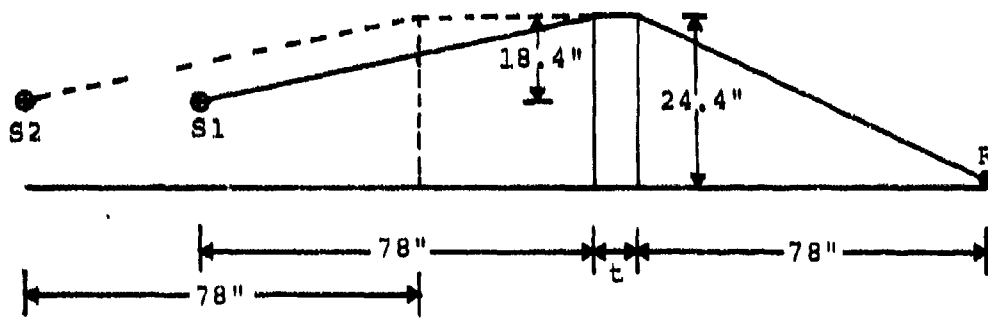
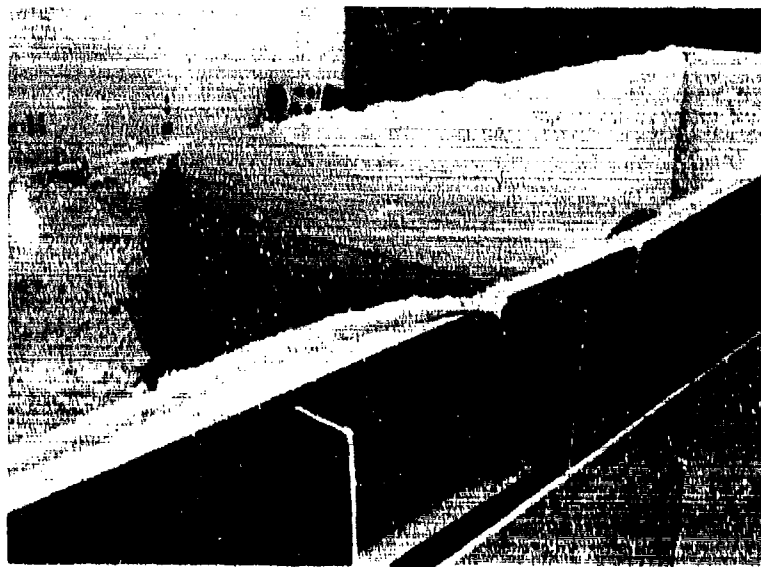


Figure 12 Setup For Barrier Tests

a-Spectrum with no walls

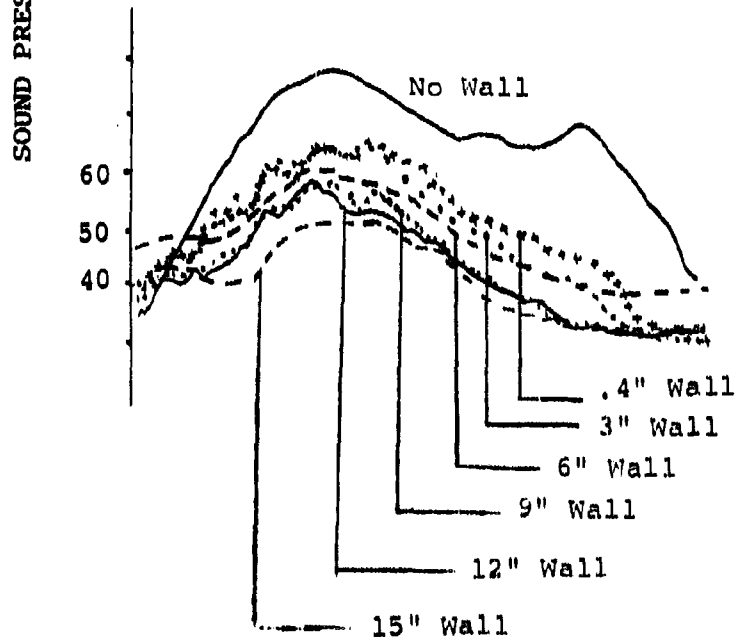
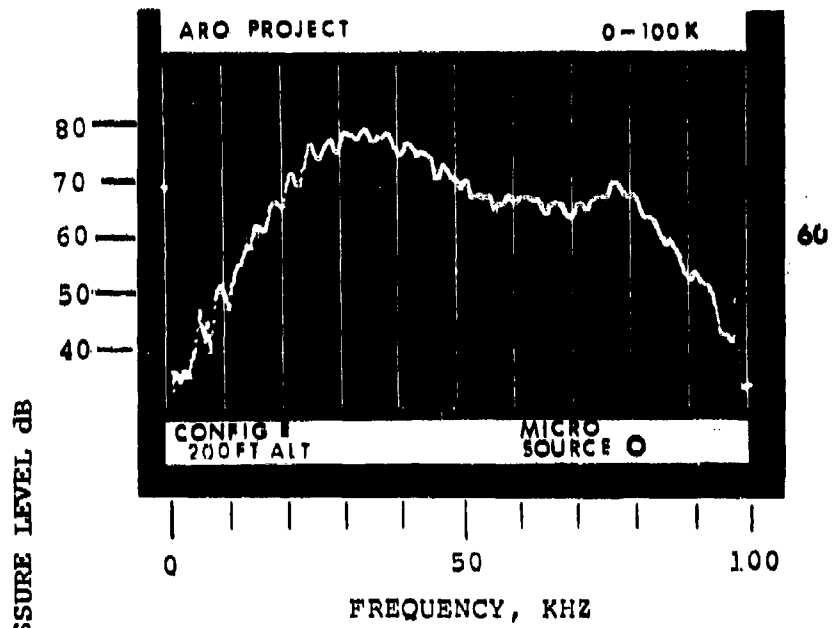


Figure 13 b-Effect of Barrier Thickness

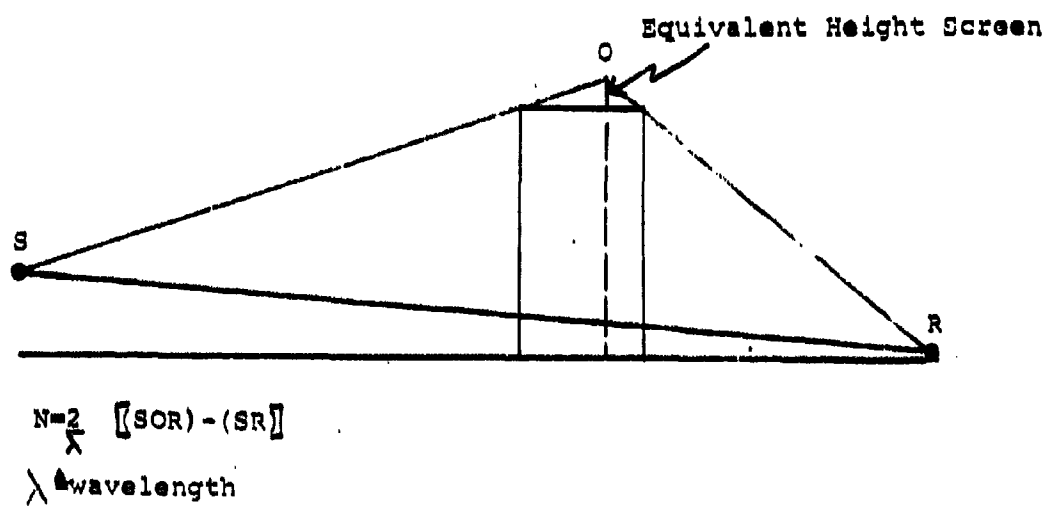
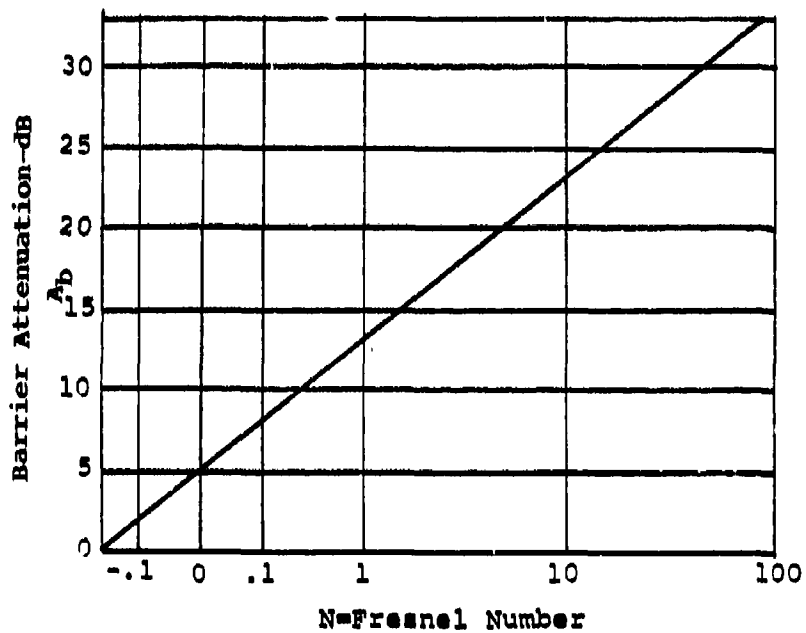


Figure 14-Prediction of Barrier Attenuation by Maekawa's Method
(Ref (6))

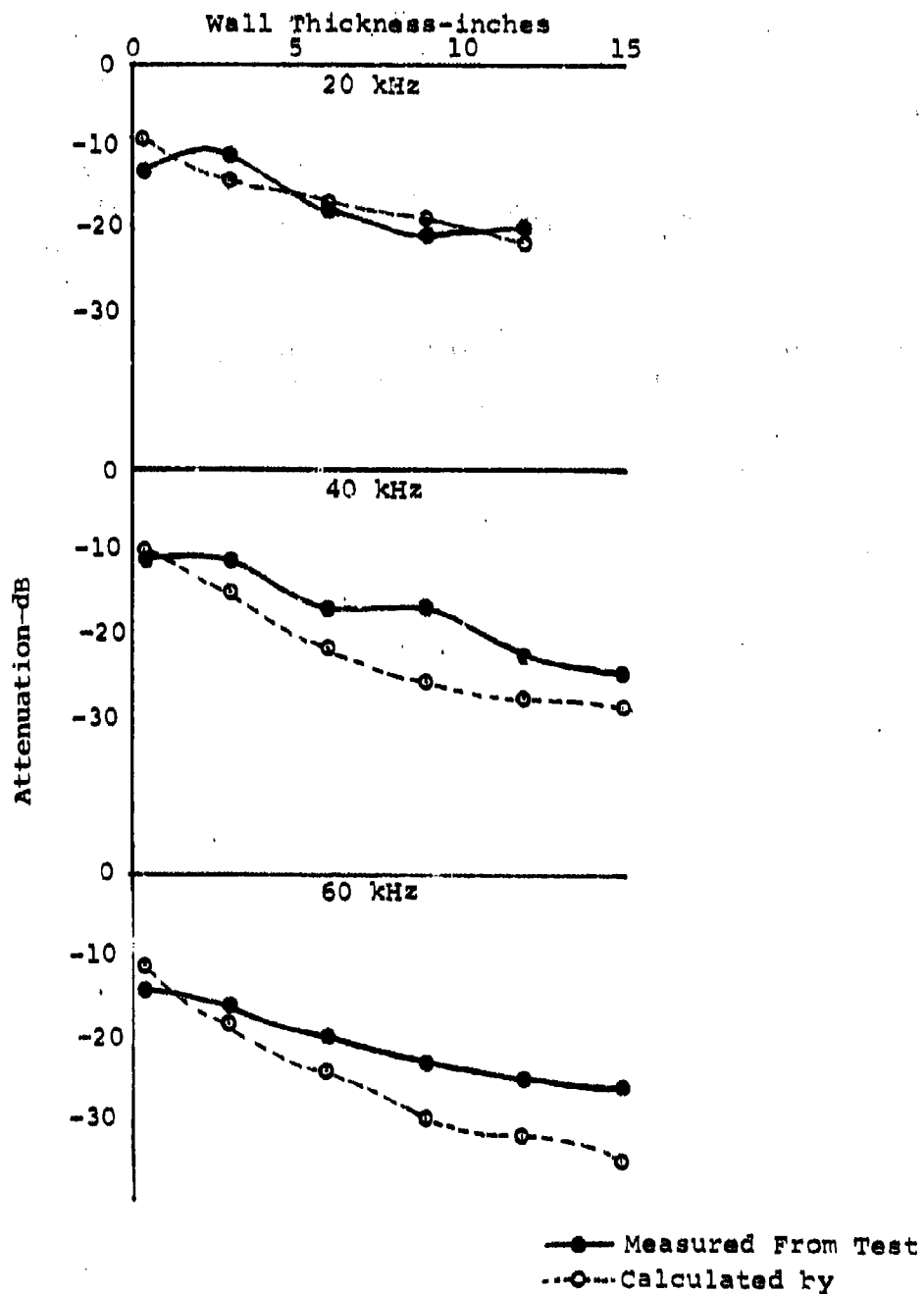


Figure 15 Comparison of Measured and Predicted Barrier Attenuation

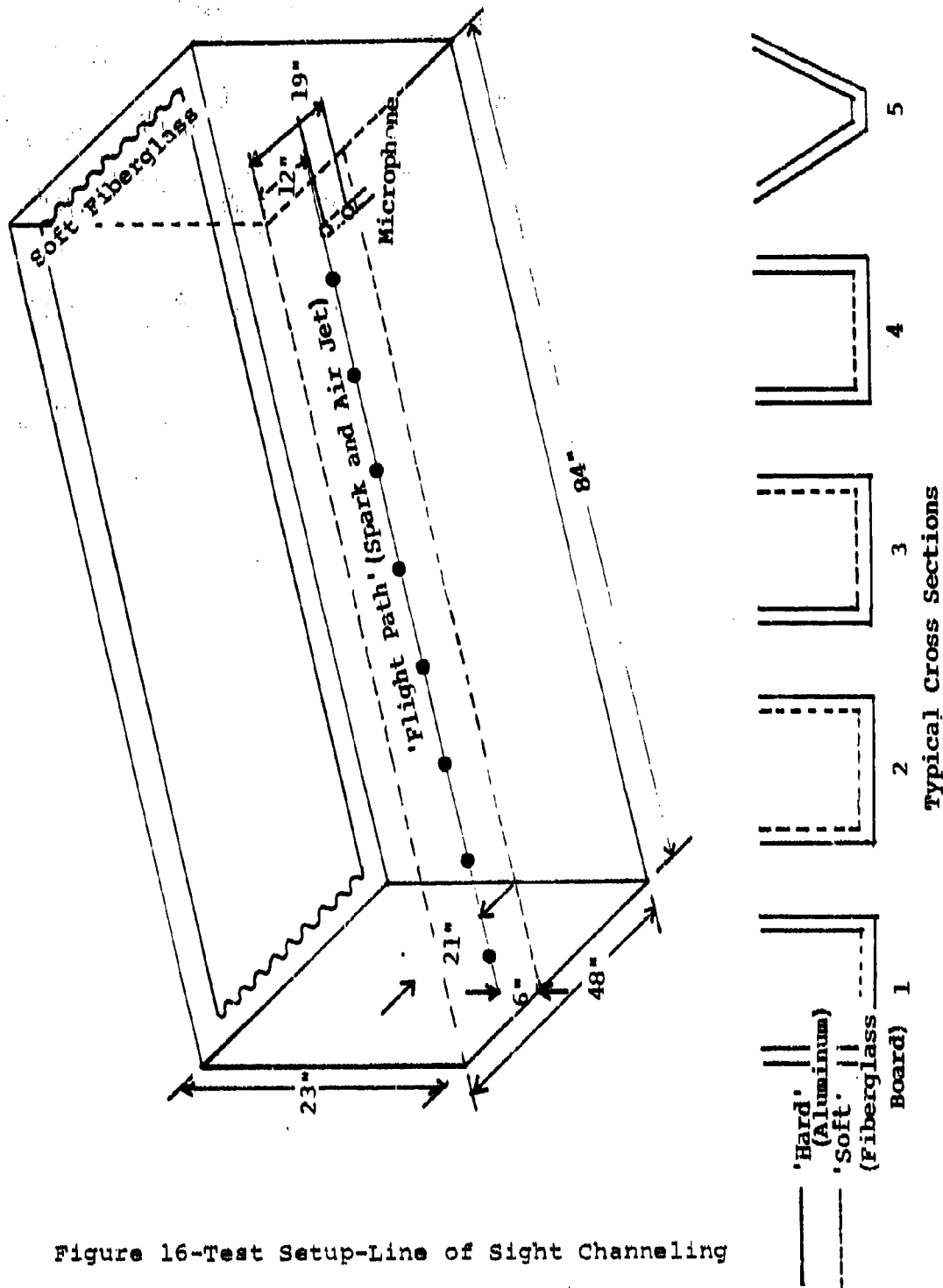


Figure 16-Test Setup-Line of Sight Channeling

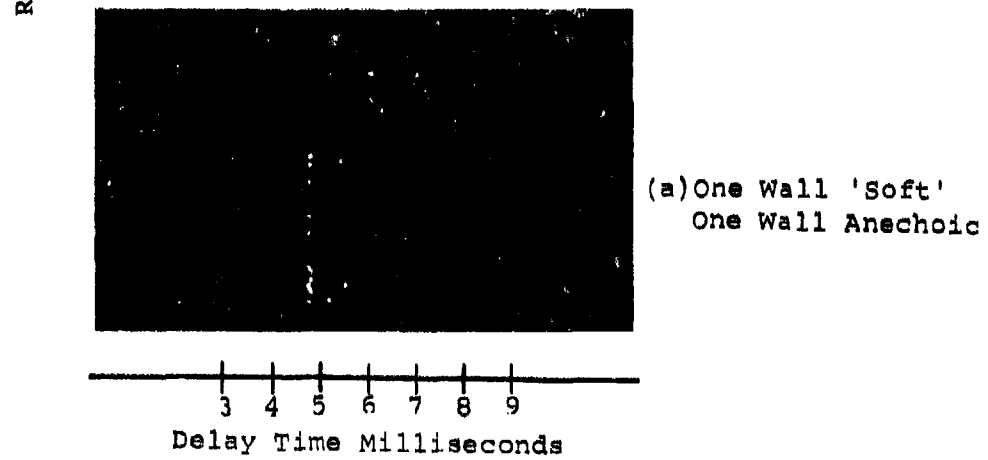
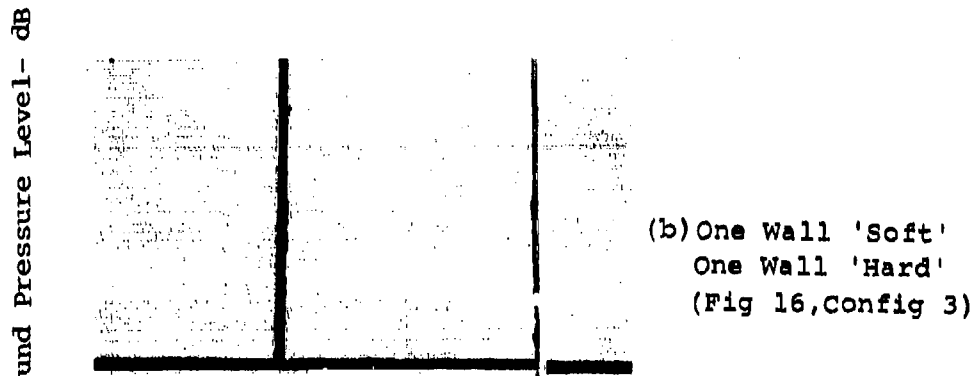
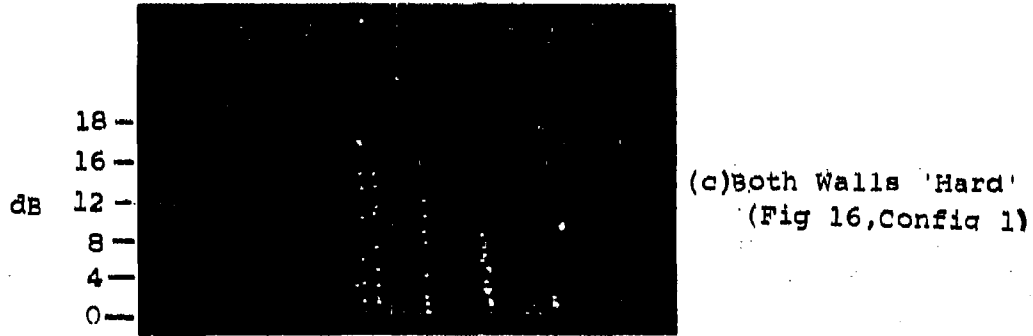


Figure 17 Typical Spark Test Results

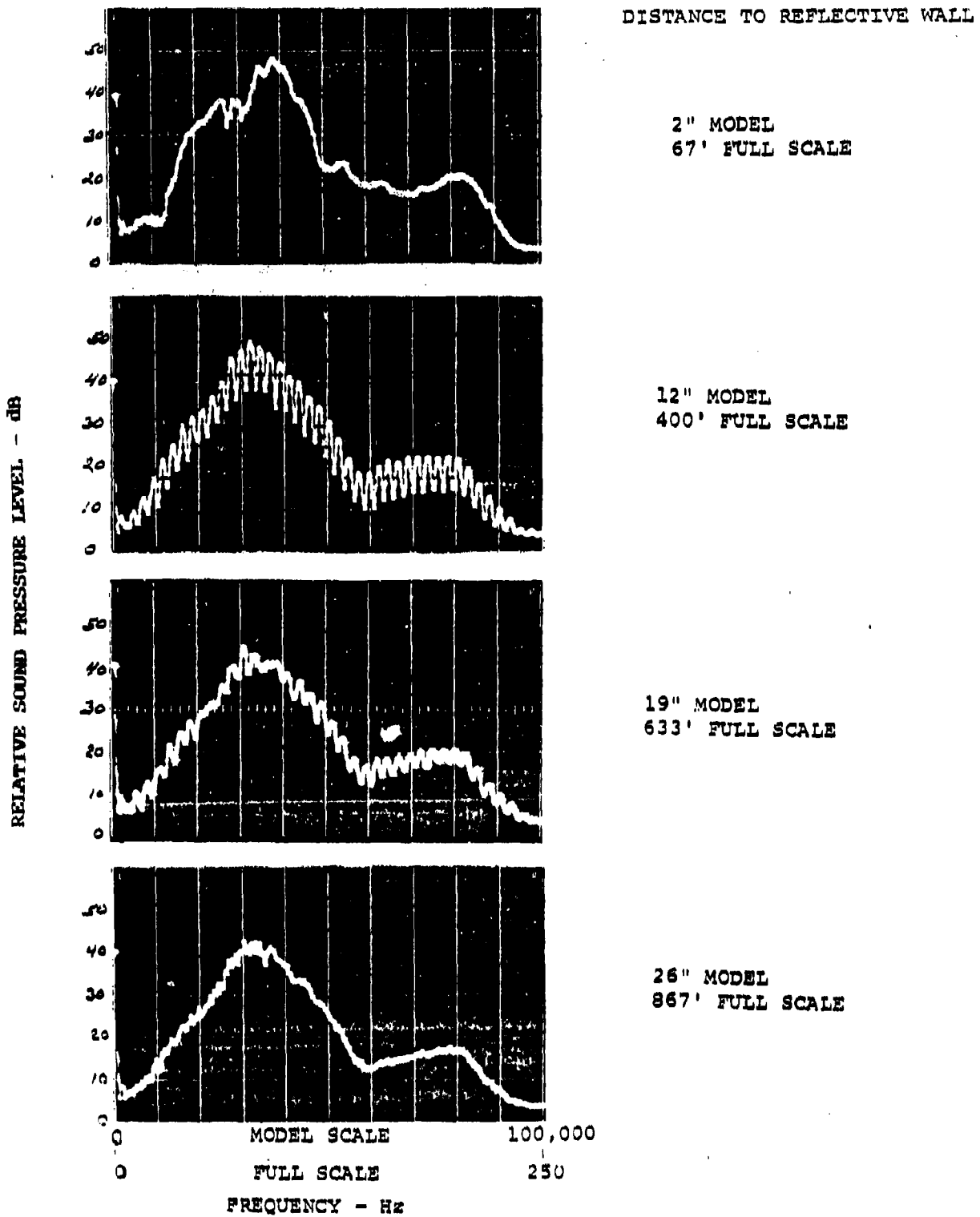
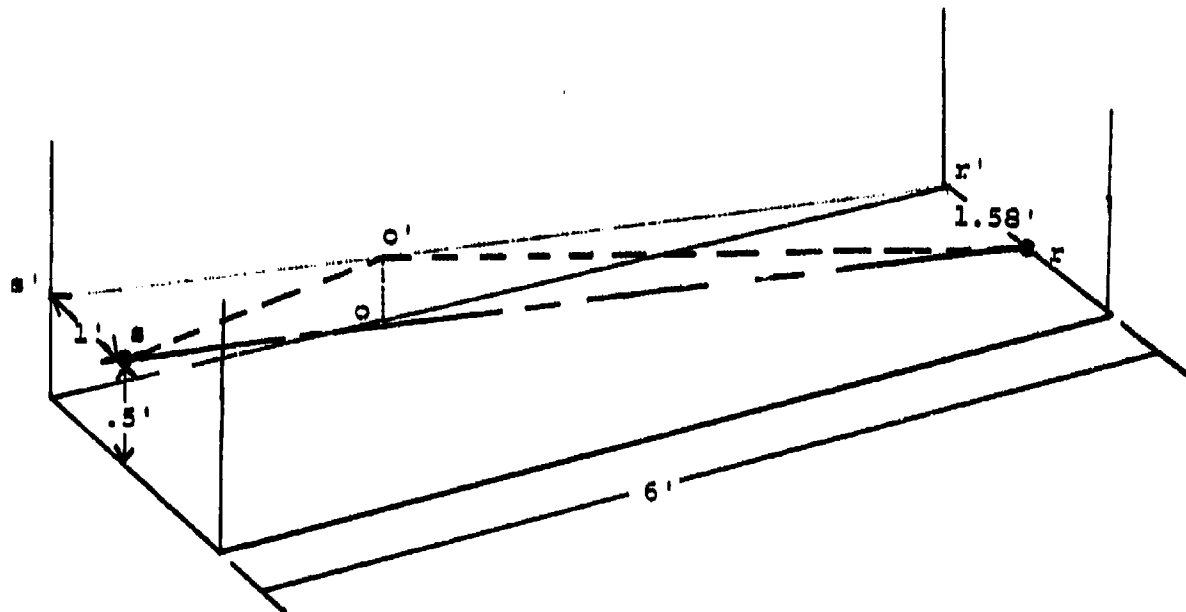


Figure 18 - Effect of Wall Distance on Acoustic Signal



$$O-O' = \frac{1.58}{2.54} \times .5 = .306'$$

$$s'r' = [6^2 + .5^2]^{\frac{1}{2}} = 6.021'$$

$$s'o' = 3.334'$$

$$r'o' = 3.667'$$

$$s'o' + o'r' = \left[(.5 - .306)^2 + 1^2 + (3.334)^2 \right]^{\frac{1}{2}} + \left[(.306)^2 + (1.58)^2 + (3.667)^2 \right]^{\frac{1}{2}}$$

$$= 6.641'$$

$$sr = \left[(.5)^2 + (1.58 - 1)^2 + 6^2 \right]^{\frac{1}{2}}$$

$$= 6.049'$$

$$\delta = [s'o' + o'r'] - sr$$

$$= .593'$$

The destructive interference between paths $O'r'$ and sr will occur at frequencies which differ such that their wavelengths have differences of .593'

$$\left(\frac{2}{\lambda} \right) - \left(\frac{1}{\lambda} \right) = \left(\frac{1}{\lambda} \right) - \left(\frac{2}{\lambda} \right) = \left(\frac{2}{\lambda} \right) - \left(\frac{1}{\lambda} \right) = .593'$$

$$\lambda = \frac{c}{f} \text{ or } f = \frac{c}{\lambda}$$

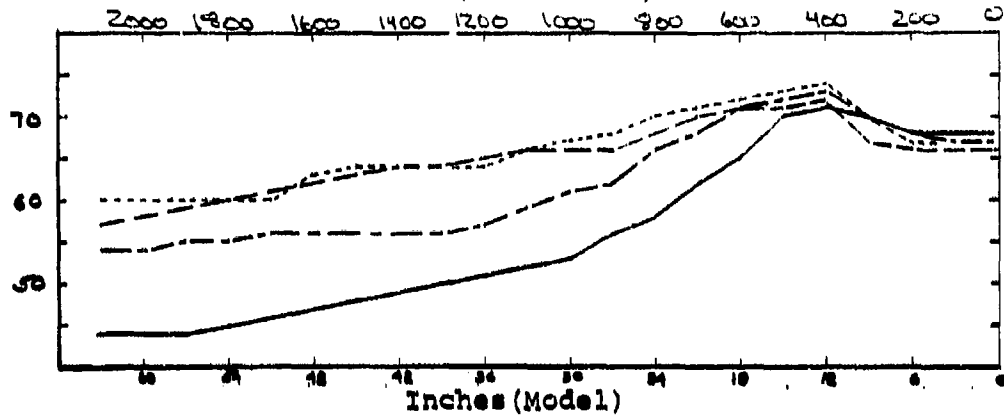
c during this experiment was 1129 ft/sec

$$\text{Interference frequency interval} = \frac{1129}{.593} = 1903 \text{ Hz}$$

Figure 19 Calculation of Interference Frequency

20 kHz-(50 Hz Full Scale)

Distance Ft-(Full Scale)



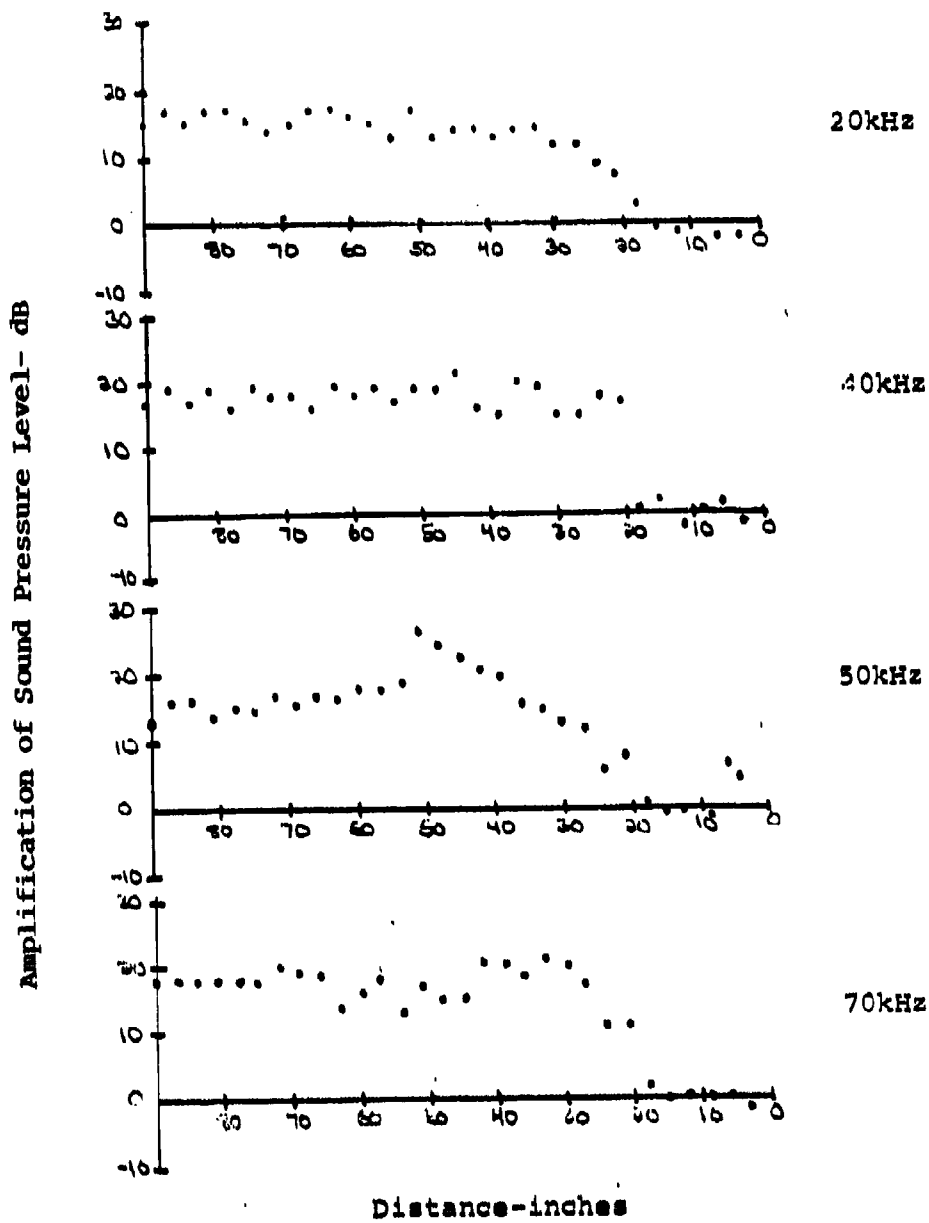


Figure 21a-Amplification-Hard Walls and Floor

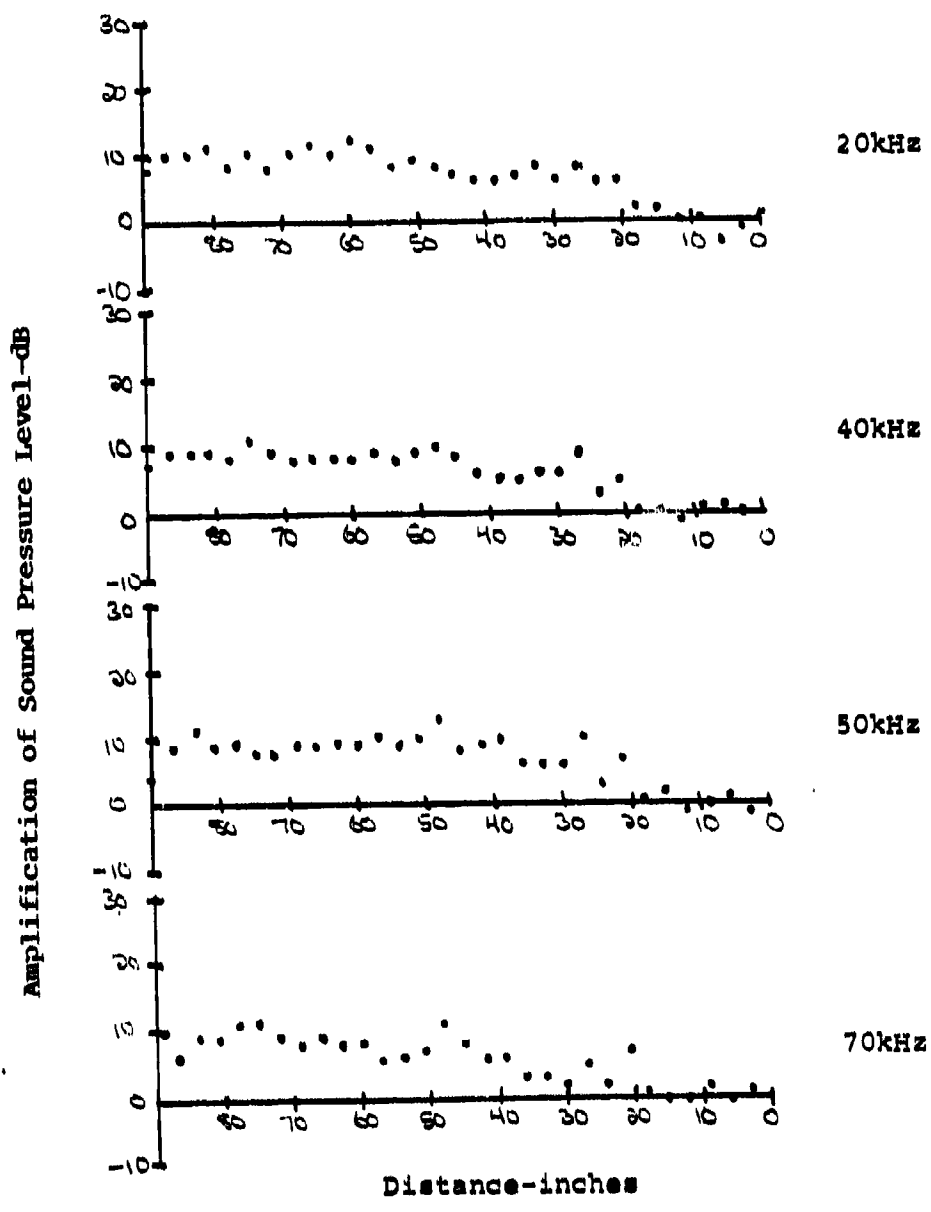


Figure 21b-Amplification-'Soft Walls', 'Hard Floor'

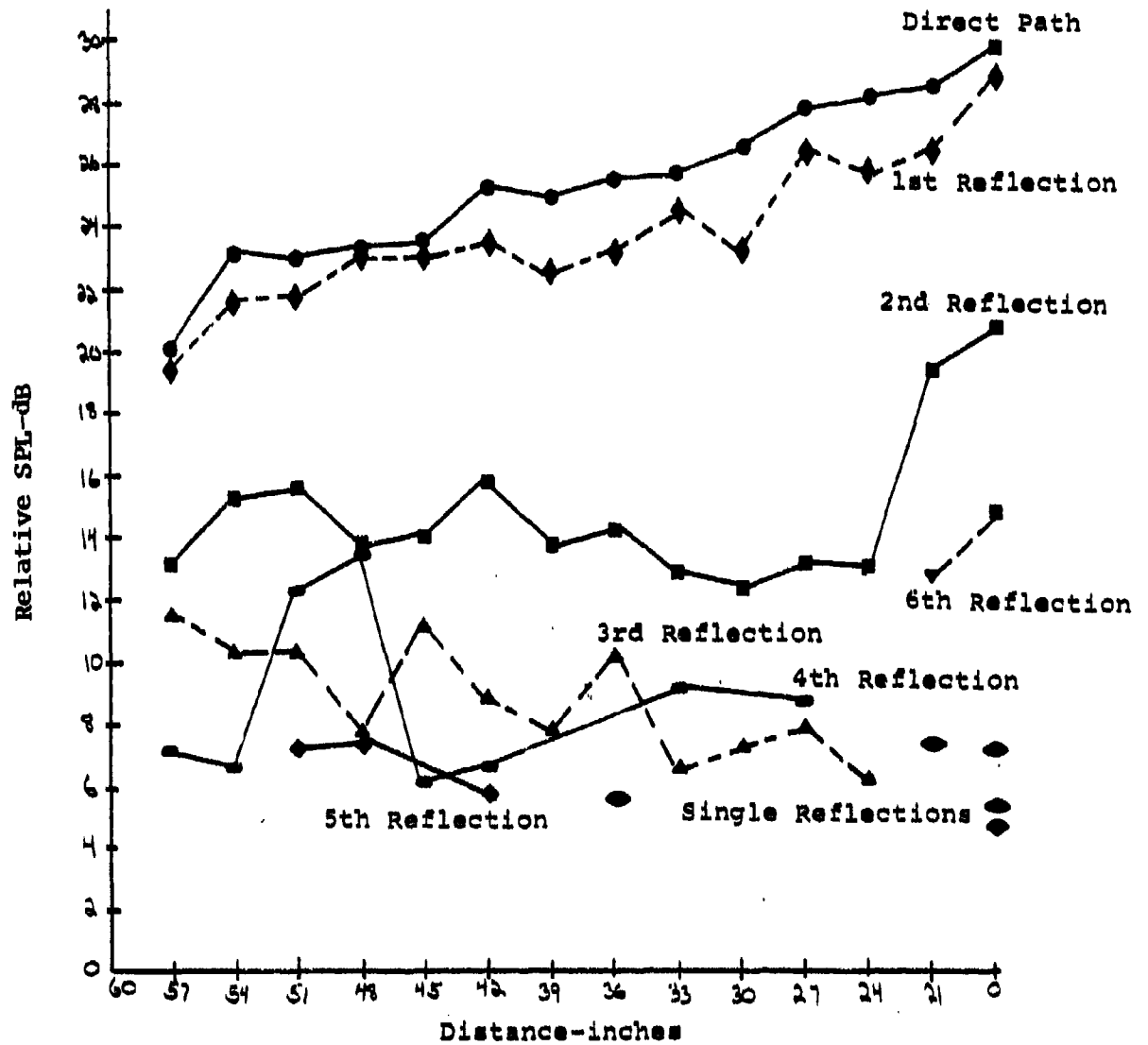


Figure 22a-Propagation Path Amplitudes Two 'Hard' Walls

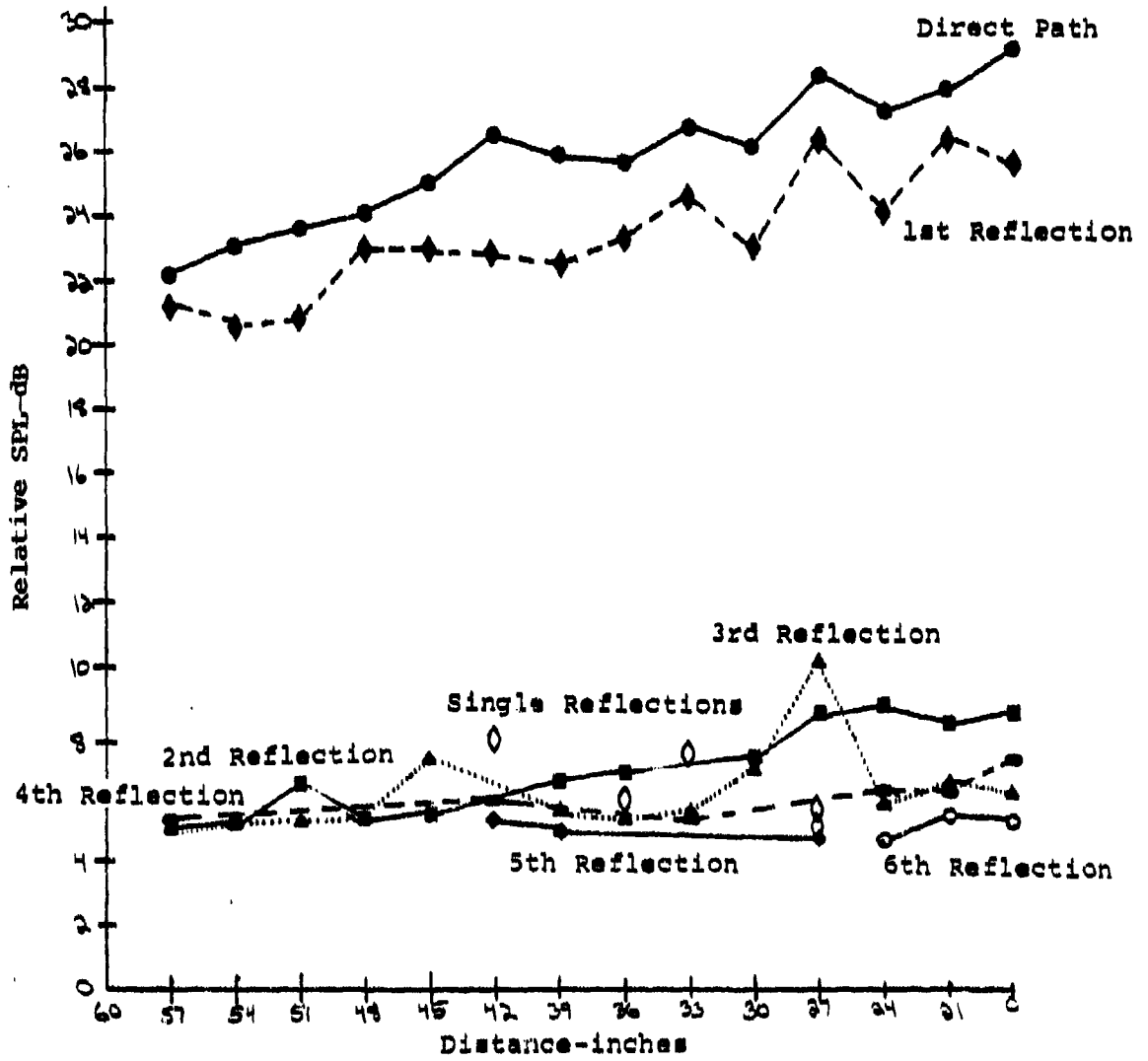
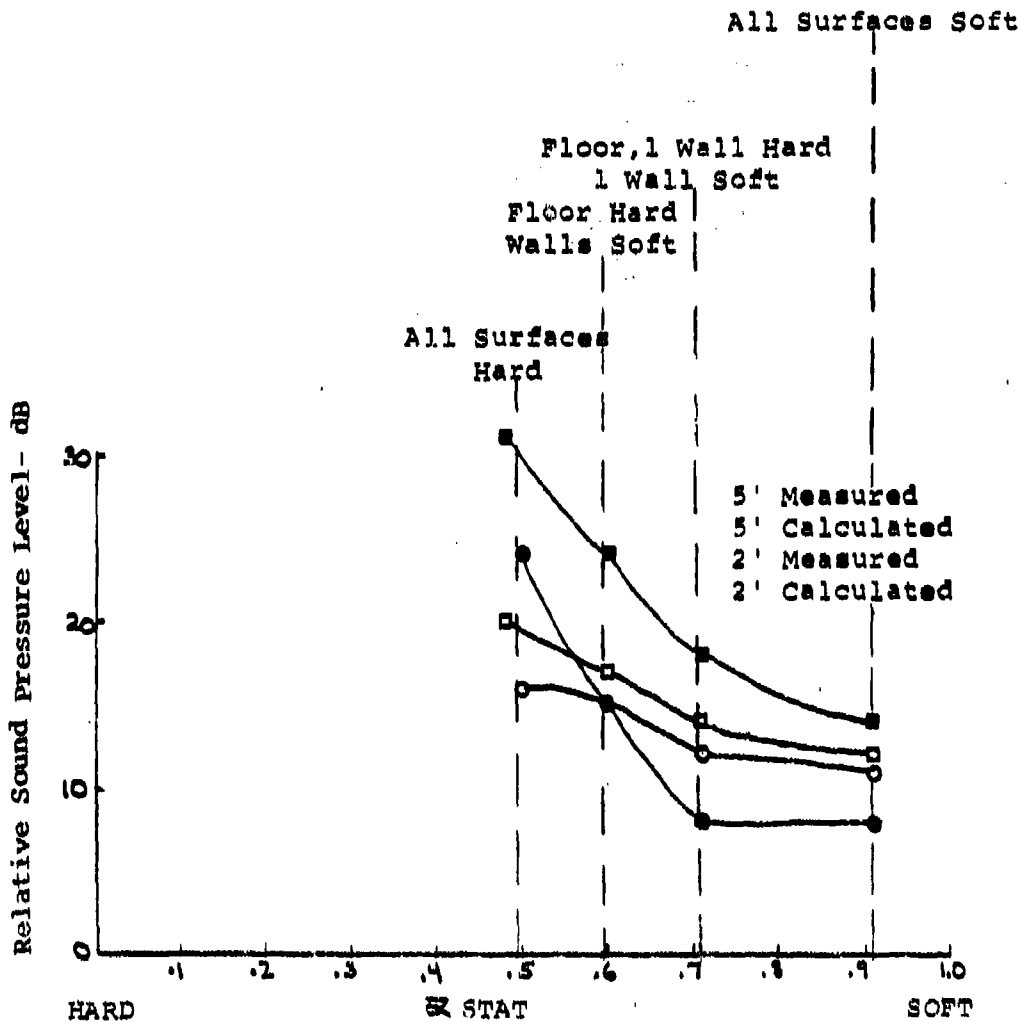


Figure 22b-Propagation Path Amplitudes One 'Hard' Wall



$$Q \text{ STAT} = \frac{\sum S_n \alpha_n}{4S_n}$$

S_n = Surface Volume of a Room Boundary
 α_n = Absorption Coefficient

Figure 23- Amplification in a Straight 'Canyon'

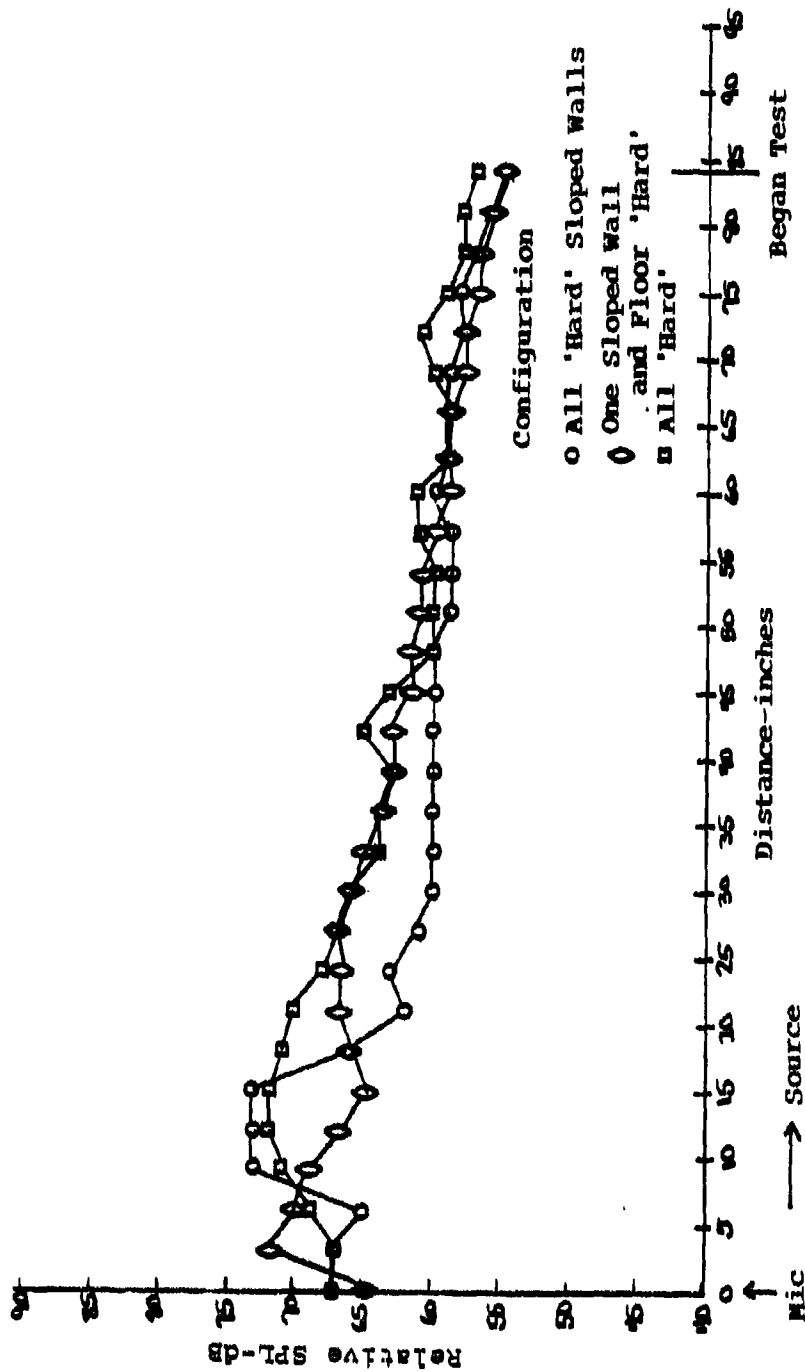


Figure 24 Effect of Wall Slope- 200 kHz

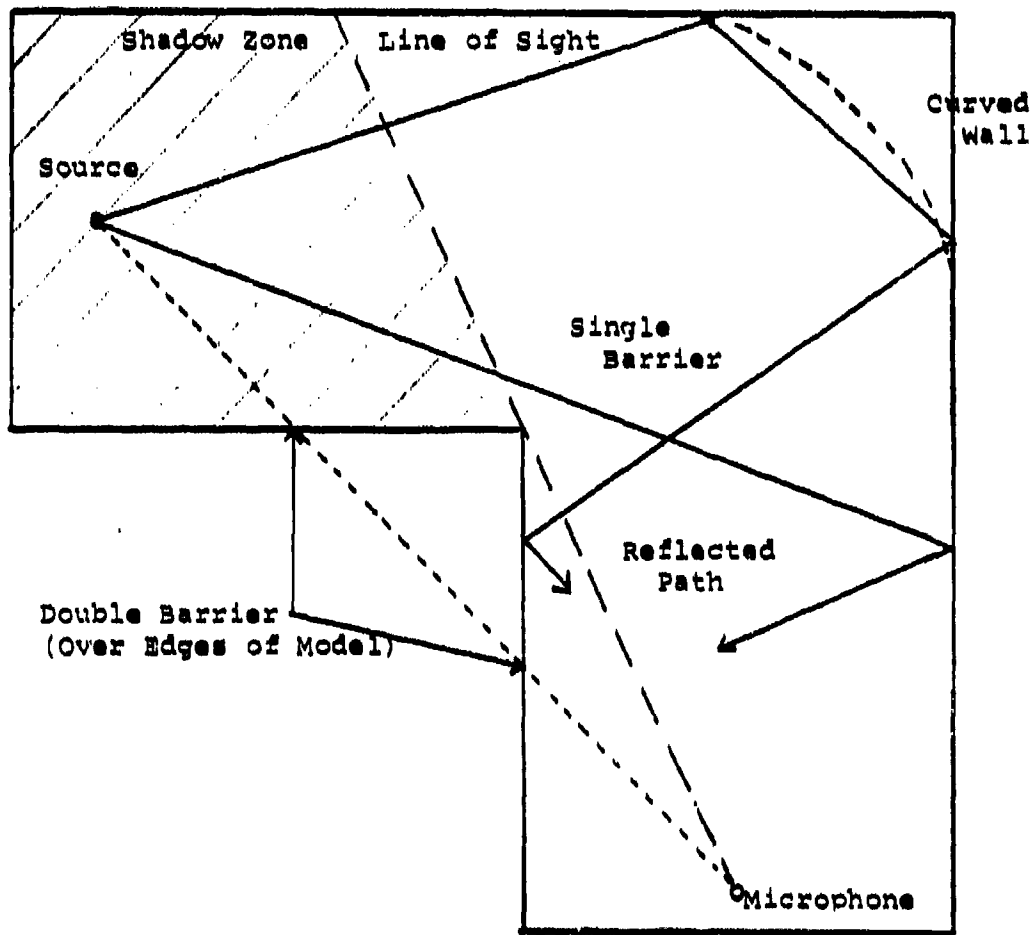


Figure 25- Bent Channel Configuration and Propagation Paths

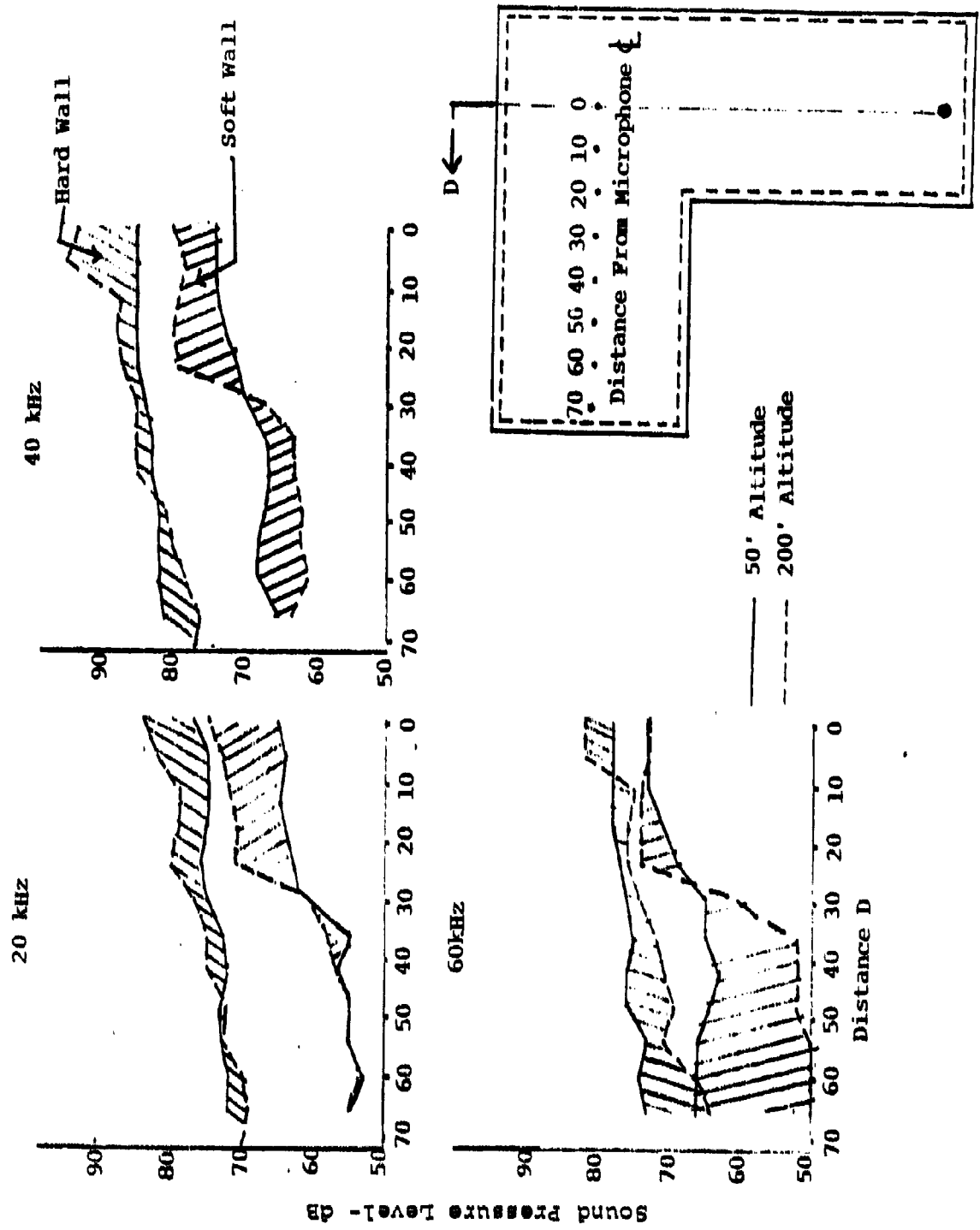


Figure 26- Effect of Wall 'Hardness'

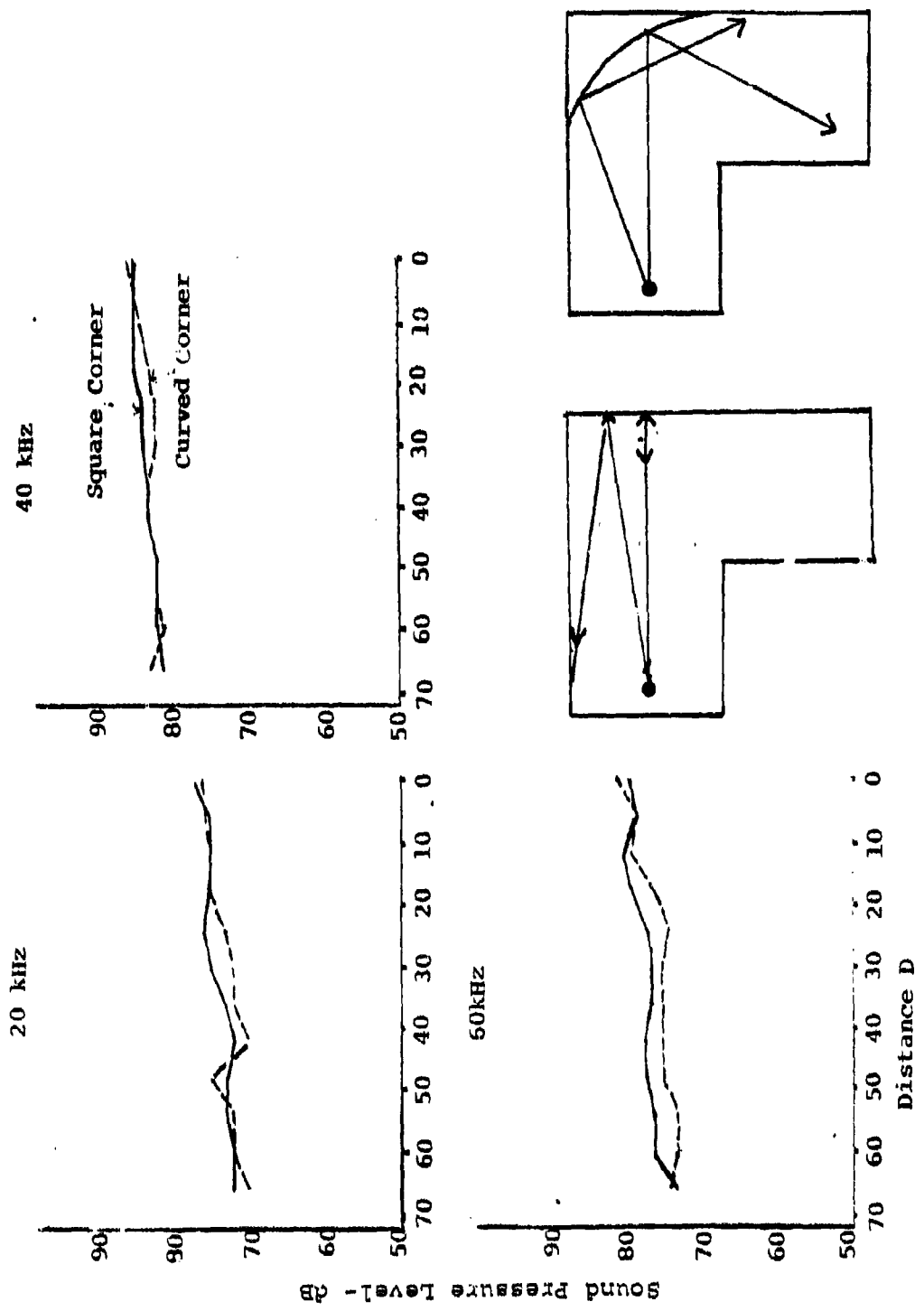


Figure 27- Effect of Curved Bend-Nap of Earth (50') Altitude- 'Hard' Walls

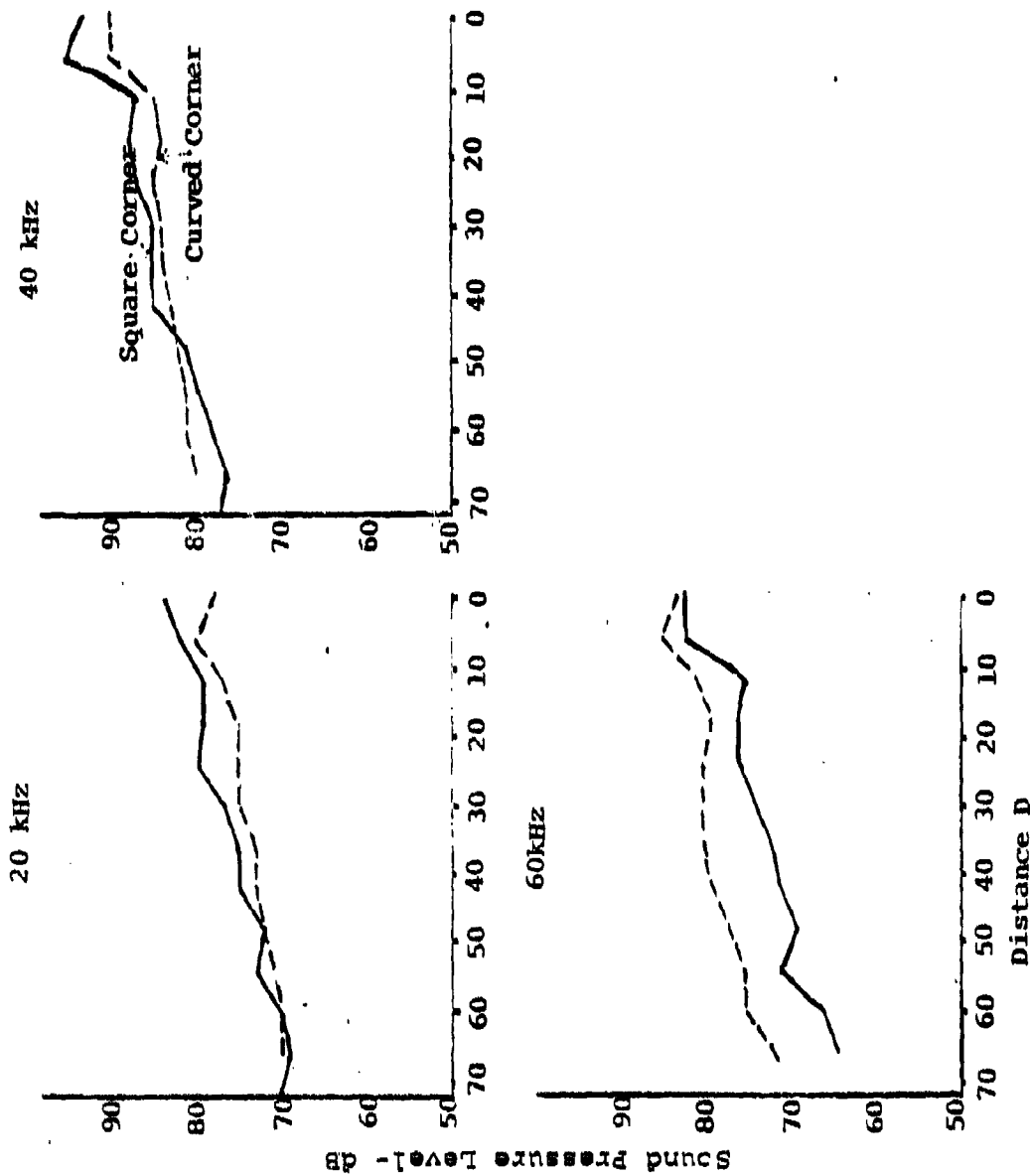


Figure 28- Effect of Bend Curvature (200'). Altitude- 'Hard' Walls

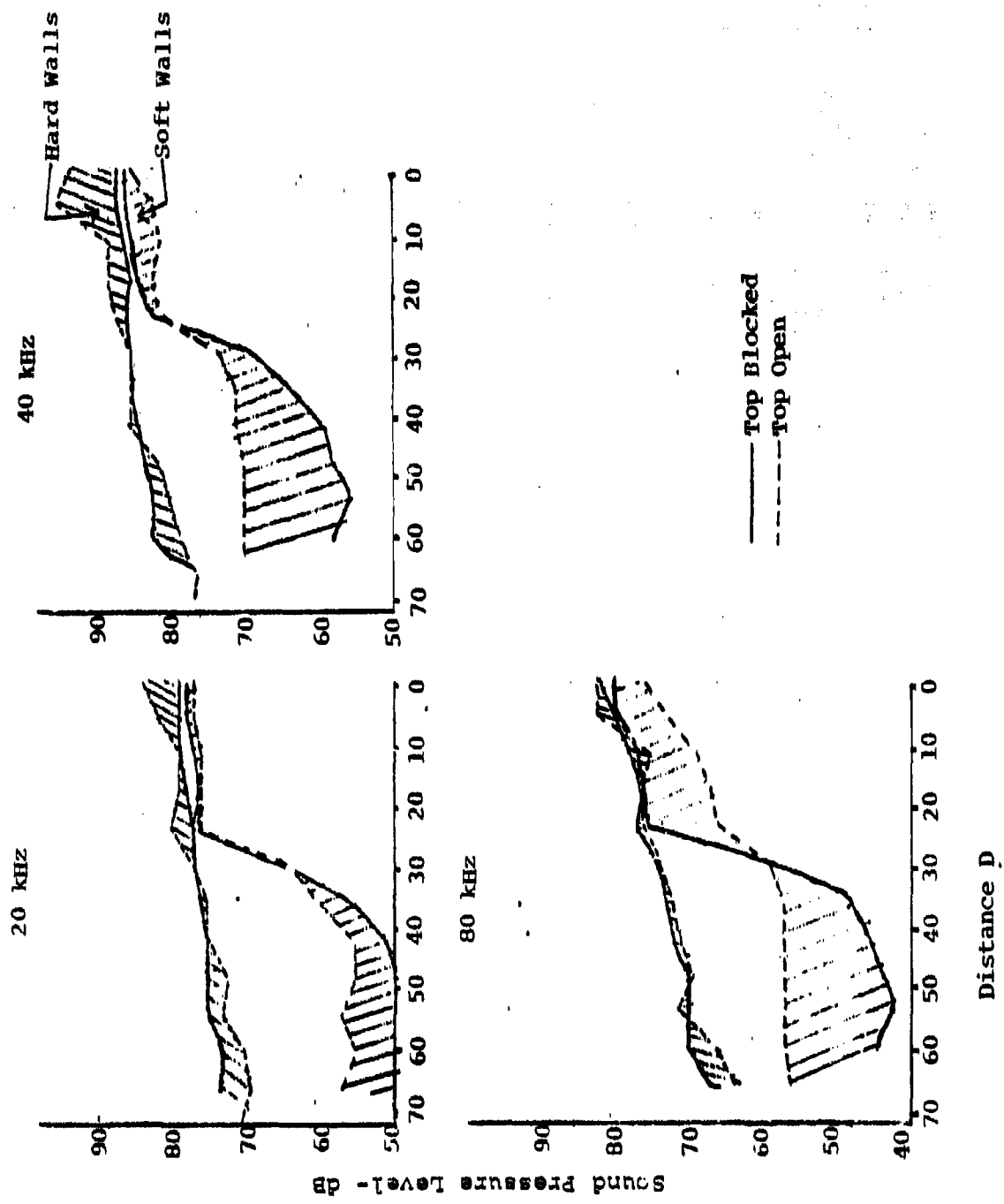


Figure 29- Propagation Over Edge of Walls